DOI:
10.1002/dvdy.24250

Document Version
Peer reviewed version

Developmental Dynamics

Understanding the development of the respiratory glands.

Journal:	*Developmental Dynamics*
Manuscript ID:	OGDVDY-14-0254
Wiley - Manuscript type:	Reviews
Date Submitted by the Author:	20-Oct-2014
Complete List of Authors:	May, Alison; King's College London, Craniofacial Development and Stem Cell Biology Tucker, abigail; King's College London, Craniofacial Development
Keywords:	pulmonary disease, signalling pathways, sinus, submucosal

Understanding the development of the respiratory glands.

Running Title: Respiratory gland development.

Department of Craniofacial Development and Stem Cell Biology, Dental Institute, King's College London, Floor 27 Guy's Tower, London Bridge, SE1 9RT London, UK.

§ author for Correspondence

abigail.tucker@kcl.ac.uk

Keywords: pulmonary disease, signalling pathways, sinus, submucosal.

This work was funded by the Dental Institute, King's College London, UK.

Abstract

The submucosal glands (SMGs) of the respiratory system are specialized structures essential for maintaining airway homeostasis. The significance of SMGs is highlighted by their involvement in respiratory diseases such as cystic fibrosis, asthma and chronic bronchitis, where their phenotype and function are severely altered. Uncovering the normal development of the airway SMGs is essential to elucidate their role in these disorders, however, very little is known about the cellular mechanisms and intracellular signals involved in their morphogenesis. This review describes in detail the embryonic developmental journey of the nasal SMGs and the postnatal development of the tracheal SMGs in the mouse. We also review the current knowledge of the genes involved in SMG organogenesis, in the hope of stimulating further research into the mechanisms required for successful SMG patterning and function.

Introduction

Airway mucus plays a vital role in maintaining respiratory homeostasis as it provides the first line of defence against airborne irritants in the nasal cavity, and is essential in the mucociliary process, ensuring no foreign particles reach the lungs. Not only does its thick consistency trap foreign particles; its protein constitution additionally contains bactericidal enzymes, reducing the risk of infection. In humans, 5% of the respiratory mucus is secreted by goblet cells, which are simple columnar cells found scattered within the respiratory epithelium (RE) (Reid, 1960). The nucleus of these cells is found basally, while the apex of the cell is rich in mucin secretory granules (Freeman, 1962). The remaining 95% of the mucus secretion is released by the nasal and tracheal submucosal glands (SMGs) that lie in the underlying submucosal layer beneath the RE (Reid, 1960).

The importance of understanding SMG development and function is increasingly emphasised as more and more evidence shows their involvement in an array of severe and life threatening respiratory diseases, with SMG hyperplasia and mucus hyper-secretion common to most (Aikawa et al., 1992; Oppenheimer & Esterly, 1975; Reid, 1960). The most common hyper-secretory diseases in which SMGs play a role are cystic fibrosis (CF), asthma and chronic bronchitis. One of the earliest steps in CF pathophysiology is the occlusion and dilation of SMG ducts, evident in third trimester neonates with CF (Ornoy et al., 1987). Infants of CF then show early onset of hyperplasia and hypertrophy of SMGs (Oppenheimer & Esterly, 1975; Sturgess & Imrie, 1982). Cystic fibrosis Transmembrane conductance regulator (CFTR), the defected gene in patients suffering from cystic fibrosis (CF), is primarily expressed in the serous cells and some of the ductal cells of the SMGs (Engelhardt et al., 1992). While this suggests a functional defect in the glands of CF patients, defects in the developmental patterning of the SMGs in a CF mouse model have also been reported, suggesting an additional role during gland initiation (Borthwick et al., 1999).

Hyperplasia of the bronchial SMGs is a well defined feature of asthma airways with gland:bronchial wall area ratio being significantly increased in both chronic asthma sufferers and those that die of sudden attack, compared to control patients (Aikawa et al., 1992; Rogers, 2004). In sufferers of chronic bronchitis, the bronchial SMGs are hypertrophic, displaying mucus hyper-secretion and an increase in mucous cells compared to serous cell counterparts (Reid, 1960; Rogers, 2008).

Considering the critical involvement of SMGs in the above respiratory conditions, little is known about the developmental and homeostatic mechanisms of the respiratory glands. To understand disease states, it is first important to have a good understanding of normal SMG development and the signalling factors, modulators and pathways involved in gland morphogenesis.

Temporal Localisation of the SMGs

The SMGs are hidden in the submucosal connective tissue running along the conductive airways of the respiratory system. Nasal SMGs are organised into various groups with names according to their location in the medial and lateral nasal cavity walls (Cuschieri & Bannister, 1974; Grüneberg, 1971), while in the trachea, SMGs lie in the submucosal layer between the cartilage rings and smooth muscle (Finkbeiner, 1999). In the mouse, SMGS are found in the upper trachea with the highest volume of tracheal glands found at the anterior boundary between the cricoid cartilage (CC) of the larynx and the first tracheal cartilage ring (C1) and extending no further than the sixth cartilaginous ring (C6) (Borthwick et al., 1999; Rawlins & Hogan, 2005). In humans these glands are also found at higher density in the anterior trachea, but are known to spread entirely through the tracheal tube all the way down to the submucosal layer of the bronchi (Borthwick et al., 1999; Sturgess & Imrie, 1982). In the mouse, nasal SMGs begin to develop on embryonic day (E) 12.5 with the appearance of the first lateral nasal gland (or Steno's gland) in the form of a single tube. The remaining subgroups of nasal SMGs then start to initiate, from different locations of the medial and lateral walls (Grüneberg, 1971). The tracheal SMGs appear postnatally as initial gland buds that then undergo morphogenesis with all tracheal SMGs initiated by postnatal day P21 (Borthwick et al., 1999; Rawlins & Hogan, 2005).

Cellular Composition of the SMGs

The SMGs boast a typical tree-like structure common to all branched organs such as the mammalian lungs, kidney, mammary glands, lacrimal glands and salivary glands. Research has shown that tracheobronchial SMGs in humans consist of three distinct domains in relation to the overlying RE: (A) the secretory region of the distal gland, (B) the medial collecting region and (C) the proximal ciliated duct (Meyrick et al., 1969; Wine & Joo, 2004) (Figure 1). The secretory region is made up of two main

secretory cell types: serous cells and mucous cells. Glandular acini, “acinus” meaning “berry” in Latin, describes the cluster of serous secretory cells found at the distal gland that surrounds a central lumen (Meyrick & Reid, 1970) (Figure 1). In the trachea, the distal serous cells make up 61% of the overall secretory cell volume, forming a liquid rich in bactericidal enzymes, making it the primary defensive cell of the airway mucosa (Basbaum et al., 1990). Serous cells produce a watery solution primarily made up of proteoglycans and bactericidal proteins such as lactoferrin and lysozyme and some mucins (MUC2, MUC7) (Finkbeiner, 1999; Klockars & Reitamo, 1975; Masson et al., 1966). Serous tubules then lead into more proximal mucous tubules with mucous cells making up 39% of the remaining secretory gland volume (Basbaum et al., 1990) (Figure 1). Mucous cells produce a thick gel containing mucins MUC2 and MUC5 and antimicrobial peptide cathelicidin (Finkbeiner, 1999). The protein consistency of mucus provides ideal lubrication and acts as a chemical barrier to the exposed epithelium. The serum and mucus secreted by these specialized cells accumulates in a non-ciliated collecting duct and is then passed through a ciliated duct into the airway lumen (Figure 1). It is generally believed that mucus is expelled into the airway through the movement of the cilia within the ducts, however no concrete evidence indicates this is the case and it is suggested that the fluid is rather moved through a means of bulk flow (Ballard & Spadafora, 2007). Once secreted into the airway, mucus is swept away from the lungs to the pharynx by respiratory epithelial cilia movement where it is either swallowed and ingested, or is removed from the body by sneezing or coughing.

The Nasal SMGs and Their Secretions

The nose is one of the initial entry points of inhaled air into the respiratory system. Therefore, the epithelial lining cells of the upper respiratory tract are exposed to the highest concentrations of inhaled toxins and debris. It is the anterior nasal SMGs, along with the goblet cells of the RE that provide the first line of defence within the airway. The function of these respiratory glands is to secrete mucus into the nasal cavity where it traps airborne pathogens within inspired air, preventing them from progressing to the lower airway tubes and lungs. These mucous secretions also play an important role in warming and humidifying air, preventing the drying out of the delicate respiratory tissue. The nose is the principal organ for sense of smell, and it is also believed that the mucus produced by the nasal SMGs dissolves odorant

molecules to help them be picked up by olfactory receptors (Getchell & Getchell, 1992). Unlike humans, mice are obligate nasal breathers, therefore the nose and nasal environment of these animals are critical in maintaining respiratory health and homeostasis. For that reason, they provide an ideal model to study respiratory nasal gland development and function.

The Nose

In order to understand the developmental locations and progressions of the anterior nasal glands, the structure of the nose must be understood. In humans and rodents, the nose can be divided into three main areas known as the vestibule, the respiratory region and the olfactory region (Figure 2). The nasal vestibule is the opening site of the nose and is lined with a stratified squamous epithelium. Moving into the nasal cavity a transition into a RE occurs (Figure 2). Gross et al. (1982) showed that in mice the RE accounts for 47.5% and 45% of the total surface area of the nasal cavity in 7 week and 16 week old mice respectively. The periphery of the RE stops suddenly and the epithelium becomes olfactory in nature. In the same study the olfactory epithelium (OE) accounted for 45% and 47% of the nasal surface area in 7 week and 16 week old mice respectively (Gross et al., 1982). The primary function of the RE is to moisten and protect the cavity while the OE houses an enrichment of olfactory receptor neurons, required for the sense of smell (Popp & Martin, 1984; Purves et al., 2004). The RE and OE are supplied with mucosal secretions by goblet cells and the respiratory SMGs, and the Bowman's glands respectively (Bojsen-Moller, 1964; Frisch, 1967).

To appreciate the morphology of the nasal cavity, the capsule can be divided into the medial and lateral walls (Figure 2, B and C). The medial wall of the cavity is a simple plane of tissue that covers either side of the cartilaginous nasal septum (Figure 2, C). Shelves of bone known as conchae or turbinates curve the lateral wall of the cavity (Figure 2, B and C). The most anterior shelf is referred to as the superior concha, the middle shelf as the medial concha while the lower shelf is called the inferior concha (Figure 2, B and C). By protruding from the lateral wall, these conchae create channels within the nasal chamber over which air can flow. These channels are known as meatuses and adopt the same name as their overlying concha (Figure 2, B and C). Additionally, there are four pairs of connected air filled cavities found in the

nose, known as the paranasal sinuses (Figure 2, C). The lining of these spaces is continuous with the nasal RE and OE and secretions are drained directly or indirectly into the nose (Figure 2, C, black dotted line). The maxillary sinus is the largest of the sinuses and is located lateral to the main nasal chamber (Figure 2, C). The frontal sinuses are the second largest of the group and are found above the eyes, and between the eyes lie the ethmoidal sinuses (Figure 2, C). A fourth pair of sphenoid sinuses is found behind the eyes and nasal cavity. The function of the paranasal sinuses is disputable however it is believed they decrease the weight of the skull as well as warming and humidifying inspired air with their mucosal secretions. In contrast to humans, mice have been reported to have only anterior and posterior ethmoidal sinuses, a true maxillary sinus, a secondary maxillary sinus, as well as observable sphenoid sinuses (Jacob & Chole, 2006). SMGs are only found to drain into the true maxillary sinus in mice (Jacob & Chole, 2006), and unlike humans, this cavity is not completely closed off by the maxillary bones (Phillips et al., 2009). Despite these anatomical differences however, the rodent maxillary sinus provides a useful tool in investigating sinus SMG development and function.

Morphology and Development of the Anterior Nasal SMGs

In the mid-twentieth century, researchers analysed and delineated anterior nasal SMG topography and physiology (Bojsen-Moller, 1964; Brunner, 1942), however modern investigation of these respiratory glands is severely lacking. It has been referenced in the literature that Broman (1921) first described the topography of the anterior nasal glands and created plastic reconstructions of the glands and ducts of rodents (Bojsen-Moller, 1964; Grüneberg, 1971). According to the manuscripts published in the mid-twentieth century, it was Broman (1921) who categorised and named the nasal glands into different groups based on their location and timing of when they first arose (Bojsen-Moller, 1964; Grüneberg, 1971). Although mentioned and reviewed in these early anatomical studies, the work of Broman has been described as “lost in recent literature” (Bojsen-Moller, 1964). Despite this, his primary names and descriptions of the glands have continued throughout the years and his work undoubtedly provided the backbone of future research on anterior respiratory gland development. While previous studies have named and described the temporal location of the glands in mice, and other mammals (Brunner 1942; Bojsen-Moller 1967; Moe & Bojsen-Moller 1971; Bojsen-Moller 1964), these manuscripts fail to give descriptive explanations

and illustrative aids to help the researcher locate and differentiate all groups of glands. The aim of this review was to thoroughly investigate and describe the patterning of the anterior nasal glands and the tracheal SMGs in a mouse model, in the hope of clarifying the development and arrangement of the glands and encourage future research into their cellular and molecular behaviours.

Lateral Nasal Gland 1 or the Steno's Gland

The lateral nasal gland 1, more commonly called the Steno's Gland, is the largest of the nasal glands (Grüneberg, 1971). The gland is located beneath the wall of the maxillary sinus and releases its product into an extremely long excretory duct, which opens into the nasal cavity near the nasal vestibule. The Steno's gland, analogous to the anterior nasal gland in humans, is classified in some animals as solely serous in nature however in others it is seromucous (Moe & Bojsen-Moller, 1971; Bojsen-Moller, 1967). In dogs the Steno's gland is considered to play a principal role in thermoregulation while in marine birds it is primarily a salt gland (Butler, 2002; Wells & Widdicombe, 1986). Studies in rodents have elucidated that its secretion contains bactericidal proteins indicating an essential role in airway protection (Moe & Bojsen-Moller, 1971).

Between E12.0 and E12.5 the Steno's duct buds from the anterior respiratory epithelium (REA) on the septal side at the nasal vestibule (Figure 3, A-D). The budding of the duct occurs as the pseudostratified REA dips inwards and invaginates into the underlying mesenchyme (Figure 3, A-D). As the bud arises, an indentation in the REA is formed (Figure 3, C-D). At E13.5 duct elongation proceeds over the superior nasal meatus and distally extends through the mesenchyme of the middle concha (Figure 3, E-H). The REA indentation continues as the Steno's duct lumen, simultaneously with the growing duct. This was described by Grüneberg (1971) however no histological or illustrative description was provided. A day later at E14.5, the distal tip of the duct has reached the mesenchyme below the RE of the maxillary sinus cavity (Figure 3, I-L). At this location, duct elongation ceases and the Steno's gland begins to branch distally over the next 24 hours (Figure 3, J - red brackets). At E15.5, the extending gland branches and end buds are apparent (Figure 3, M-N). Branching of the Steno's gland continues over the next few days of embryonic development. The first sign of acinar cell differentiation is observed at E16.5 by Alcian Blue stained mucus within acini. Continual branching proceeds at E17.5, when

the gland expands (Figure 3. O-P). At this stage the majority of acinar cells are producing mucus as indicated by Alcian Blue staining in the gland (Figure 3, O-P).

The Lateral Nasal Glands

The lateral nasal glands (LNGs) are found throughout the lateral wall of the nasal chamber. Similar to the Steno's gland they have long ducts that open into the airway lumen close to the nasal vestibule, however, these glands are found within the submucosa of the lateral wall at more caudal locations. Up to 40 lateral nasal glands have been described in rabbits while approximately 20 have been reported in adult mice (Bojsen-Moller, 1964; Broman, 1921), however, it is unclear in this report how the glands were counted. From our studies, we observe five LNGs (Steno's gland and LNG2-5), which bud and elongate during embryonic murine development. This suggests that either additional LNGs initiate postnatally, or that the large number of glands previously described in adults represent branches associated with the same gland. All of these LNGs bud from the posterior respiratory epithelium (REP) that covers a lip of tissue that protrudes from the rostral end of the middle concha (Figure 4). LNG2 is the first to undergo bud initiation between E13.5 and E14.0 from the REP at the nasal vestibule closest to the nares (Figure 4 and Figure 5, B-D). Unlike the Steno's gland duct, which dips into the underlying mesenchyme forming a dent in the REA, the budding of LNG2, and all the other LNGs, involves the invagination of a solid swelling of cells from the REP into the mesenchyme. At E14.5, LNG2 caudally extends as a solid cord of cells through the mesenchyme of the middle concha (Figure 5, F-H). At this stage LNG3 is observed to be at the late bud stage, having extended slightly from the REP at a location anterior to the distal tip of the extending LNG2 duct, and lies just beneath the opening of the Steno's duct into the airway lumen through the REA (Figure 4 and Figure 5, F-H). Additionally at E14.5, LNG4 and LNG5 are observed budding from the REP covering the most rostral side of the middle concha lip, and caudal to the distal end of the LNG2 duct respectively (Figure 5, F-J).

By E15.5, the duct of LNG2 reaches its final destination beneath the maxillary sinus, above the branching Steno's gland (Figure 5, K-M). The duct of LNG3 elongates parallel to that of LNG2, with its distal tip found rostral to the end of the arrested LNG2 duct (Figure 5, K-M). LNG4 elongates posteriorly through the middle concha

and its distal tip emerges in the mesenchyme below the enclosing cartilage of the nasal capsule (Figure 5, N-O). This suggests that LNG4, although structurally similar to the other LNGs, could be following a different molecular signal that attracts its elongating gland duct in a posterior direction, compared to a caudal attractant guiding the other LNGs. Regardless of this difference in spatial-temporal development, all the LNGs appeared to follow the same pattern of cavitation and branching morphogenesis. The LNG5 duct elongates caudally through the middle concha and arrests rostral to the ends of LNG2 and LNG3 (Figure 5, K).

By E16.5, LNG2 has branched distally above the Steno's gland, showing the formation of end buds (Figure 6, A-B). The beginning of lumen formation within the acini of LNG2 is apparent at this stage (Figure 6, B – white arrows). No mucus production is evident in acinar cells of LNG2 at this stage. The distal tip of LNG3 duct has reached the caudal end of the middle concha, where it was found lying rostral to the branching LNG2 (Figure 6, A-B). LNG3 has begun branching morphogenesis as the first signs of end buds are observed (Figure 6, B – green arrows). LNG4 is at a similar stage of development with the formation of end buds noted at its distal end below the nasal cartilage capsule (Figure 6, E-F). The duct of LNG5 has elongated through the middle concha beneath the RE, parallel to the ducts of LNG2 and LNG3, where it begins branching over the next 24 hours (Figure 6, I-J).

By E17.5, LNG2 has undergone extensive branching and cells have arranged into distinct acini (Figure 6, C-D). The distal gland of LNG3 has also undergone similar branching and clear lumens are identified within acini (Figure 6, C-D). No mucus staining by Alcian Blue is evident at E17.5 in both the LNG2 and LNG3. LNG4 has formed numerous branches and terminal end buds and cavitation has begun within acini (Figure 6, G-H). LNG5 has begun to form distal epithelial gland buds and lumen formation has progressed from the duct to acini (Figure 6, K-L)

The Medial Nasal Glands

The medial nasal glands (MNGs) are found within the submucosa of the medial wall on either side of the septum. Their long ducts open at rostral locations while their glands progress caudally and are seen anterior to the vomeronasal organ in rodents. These glands have been previously described in the rat, which can have four to five MNGs that project into the septal mesenchyme (Bojsen-Moller, 1964). The MNGs

have been reported as having serous acini by light microscopy (Kerjaschki, 1974). The rat MNGs do not stain with Periodic-Acid Schiff (PAS) or Alcian Blue staining (Bojsen-Moller, 1964). Analysis of the four MNGs of the mouse have also been carried out (Broman, 1921; Kerjaschki, 1974). These glands have previously been reported to be exclusively made up of serous cells (Bojsen-Moller, 1964; Kerjaschki, 1974) and in our studies, no Alcian Blue staining is seen within their acini during embryonic stages, suggesting these glands are exclusively serous in nature. While all the MNGs look similar and undergo comparable developmental strategies, investigation into their ultrastructure has delineated distinguishable differences between these glands (Kerjaschki, 1974). It has been shown that MNG4, shows homologous characteristics to serous salivary glands, with its gland cells having common characteristics as serous cells, however MNG1-3 stand alone as their own distinct gland type (Kerjaschki, 1974). What differentiates MNG1-3 from the fourth is that they possess “light” and “dark” endpiece cells within their glandular acini when analysed by electron microscopy (Kerjaschki, 1974). These “light” and “dark” cells have been described in the Bowman’s glands of the olfactory epithelium, where “light” cells contain electron-dense serous secreting vesicles while the “dark” cells contain electron-lucent mucous secreting vesicles (Getchell & Getchell, 1992). These compositional differences of these glands may also explain why in this study we see MNG1-3 elongate and branch in the same plane and at similar time points, when MNG4 arises in the more rostral septum and develops slightly later. While all are considered ‘Medial Nasal Glands’, for future studies it is advised to be aware of their differences.

Development of the MNGs is relatively simple to follow as their ducts elongate and branch through the clear plane of mesenchymal tissue on either side of the nasal septum. All MNGs bud from the RE covering either side of the nasal septum of the medial wall and elongate and branch within the mesenchyme of the septum (Figure 7, A-L). MNG1 and MNG2 are the first to bud between E14.0 and E14.5. At E14.5 ducts of these two medial glands have elongated (Figure 7, A-D). By E15.5 these ducts have elongated into the central area of the septum while MNG3 has budded and elongated to the midline of MNG1 and MNG2 (Figure 7, E-H). Through another plane of mesenchyme it is clear that branching of MNG1 begins by E15.5 (Figure 7, inset image H). Branching progresses by E16.5 in MNG1 and end bud formation is

also underway in MNG2 (Figure 7, I-J). MNG3 elongates adjacent to the ducts of MNG1 and MNG2 at E16.5 (Figure 7, I-J) and begins branching over the next 24 hours. At E17.5, MNG1, 2 and 3 are all branching, with branches and terminal end buds all crossing over one another (Figure 7, K-L). MNG4 has also elongated and begun its branching at E17.5, indicated by the presence of end buds (Figure 7, K-L).

The Maxillary Sinus Glands

The maxillary sinus glands (MSGs) bud and branch from the RE at both the anterior and posterior walls of the maxillary sinus. They do not have long gland ducts like the other anterior nasal glands but rather branch within the mesenchyme close to the epithelium. Research on the MSG in rat found it to be an exclusively serous gland (Vidić & Greditzer, 1971) and begins its development at E16 (Vidić, 1971). In the mouse, we show that the MSGs undergo a similar method of development as in the rat, however, is first seen to bud from the epithelium of the maxillary sinus at approximately E15.0. The anterior and posterior sinus glands undergo the same developmental patterning so for expediency the development of only the posterior MSG will be explained. At E14.5, no evidence of a MSG is observed (Figure 8, A-B) however by E15.5 branching of the MSG is apparent close to the RE (Figure 8, C-D). At this stage the MSG is observed to invaginate into the mesenchyme with preformed lumens within the branching epithelium. Branching of the MSG epithelium continues over the next two days of embryonic development with lumens constantly present within the end buds (Figure 8, E-H).

Signalling During Nasal SMG Development

The Wnt signalling pathway is an evolutionary conserved pathway, critical for controlling the development of an organism. Many developmental processes such as cell proliferation, migration, polarity and fate determination rely on the regulation of Wnt signalling (Komiya & Habas, 2008). Two categories of Wnt transduction pathways are known, the canonical Wnt/β-catenin cascade, and the non-canonical Wnt/β-catenin-independent cascades, which include the Wnt/Planar Cell Polarity pathway and the Wnt/Calcium pathway. The former of these, the canonical Wnt signalling pathway, is the most studied and involves the binding of extracellular Wnt ligands to transmembrane bound Frizzled receptors and a co-receptor, low-density lipoprotein receptor related protein 5 (LRP5) or LRP6. In the absence of Wnt ligand binding, cytoplasmic β-catenin is constantly broken down by the Axin complex,

consisting of Axin, glycogen synthase kinase 3 (GSK3), casein kinase 1 (CK1) and the *adenomatous polyposis coli* gene product (APC). Together, GSK3 and CK1 phosphorylate β-catenin, rendering it recognisable to the E3 ubiquitin ligase subunit β-Trcp (Davidson et al., 2005; Liu et al., 2002; Zeng et al., 2005). Subsequent ubiquitin of β-catenin occurs, followed by its proteosomal degradation (He et al., 2004). Upon Wnt ligand-receptor binding, the Axin complex is recruited to the cell membrane bound receptor complex, preventing the β-catenin inhibitory effects of these proteins, and thus β-catenin degradation (He et al., 2004). This permits β-catenin translocation into the nucleus where it can activate Wnt-responsive genes. The most studied nuclear mediators targeted by Wnt signalling belong to the lymphoid enhancer factor 1/T-cell factor (LEF-1/TCF) family (Arce et al., 2006; Eastman & Grosschedl, 1999).

Wnt signalling negatively regulates branching morphogenesis in other branching organs (Dean et al., 2005; Patel et al., 2011). *Ex vivo* culture of lung, lacrimal and the submandibular salivary gland (SMDG) with WNT3A, leads to an inhibition of clefting and a reduction in the number of epithelial branches (Dean et al., 2005; Patel et al., 2011). Using the *Axin2*^{lacz} reporter, it has been shown that Wnt/β-catenin signalling is restricted to the ductal structures of the developing SMDG, with its localisation seen at E14.5, during the late *Pseudoglandular stage,* in the main gland duct and by E15.5 spreading into the smaller ducts (Patel et al., 2011). Wnt activity may be maintained in the ductal epithelial cells to ensure their long-range elongation before the branching of a distal gland occurs. Wnt activity is maintained in the intercalated ducts of the SMDG during postnatal development, however, reduces as mice age (Hai et al., 2010). Enhanced Wnt activity is observed in ductal cells following SMDG duct ligation, indicating a role of this pathway in SMDG regeneration (Hai et al., 2010). Using the *Lef1* -/- mouse to study the biological role of this gene, it was shown that knockout mice failed to develop organs such as teeth, hair follicles and mammary glands (van Genderen et al., 1994).

Using the β-catenin/Tcf-βgal reporter (TOPGAL) mouse, it has been shown that the canonical Wnt pathway is active during early nasal gland bud formation (Driskell et al., 2007). Additionally, the transcription factor *Lef1*, has been shown to be highly

expressed in progenitor cells of early SMG buds in the mouse nose and trachea, and the ferret trachea, and in *Lef1* knockout mice, amorphous aggregates of cells develop where nasal SMGs are seen in wild types (Driskell et al., 2004; Duan et al., 1999, 1998). *Lef1* promoter expression has been shown to be regulated by Wnt-3a during SMG morphogenesis, and in the *Wnt3-a* knockout mouse, SMG *Lef1* expression was lost and cell proliferation of epithelial gland cells was reduced in SMG buds (Driskell et al., 2007). While these studies have given insight into the necessity of Wnt signalling for early SMG bud formation, the involvement of Wnt molecules in later stages of respiratory gland development has not been investigated.

The role of the Ectodysplasin A (EDA) pathway has been investigated in the development of a number of ectodermal derived organs (Mikkola, 2009). Mutations in the Eda pathway genes in both humans and mice leads to hypohidrotic ectodermal dysplasia (HED) which gives rise to congenital defects in salivary glands, hair, teeth and sweat glands (Clarke et al., 1987). Signalling through this pathway involves the binding of EDA A1, a member of the tumor necrosis factor (TNF) family, to a death domain transmembrane receptor, EDAR (Headon & Overbeek, 1999; Srivastava et al., 1997). EDA ligand binding to EDAR leads to the recruitment of the intracellular adaptor protein EDAR Associated Death Domain (EDARADD). Recruitment of EDARADD to the receptor leads to the formation of a complex containing the cytoplasmic proteins TNF Receptor Associated Factor 6 (TRAF6), TGF-β Activated Kinase 1 (TAK1) and TAK Binding Protein 2 (TAB2) (Morlon et al., 2005). This leads to the activation of the IκB kinase complex (IKK), which is a compound of two kinase sub-units, IKK1 and IKK2, as well as the regulatory component NF-kappaB essential modulator (NEMO) (Döffinger et al., 2001; Morlon et al., 2005). Activation of the IKK complex triggers recruitment and the phosphorylation of inhibitor kappa-B (IκB), a nuclear factor-kappaB (NFκB) inhibitor. Phosphorylation of IkB leads to its degradation, and NFκB translocates into the nucleus where it acts as a transcription factor, regulating target genes involved in cell proliferation, differentiation and survival (Gilmore, 2006; Oeckinghaus & Ghosh, 2009).

A number of reports using the mouse model have shown the importance of Eda signalling in both major and minor salivary gland morphogenesis. Analysis of the *Tabby* mouse, a model of a naturally occurring mutation in the gene required for EDA

(Srivastava et al., 1997), gave rise to hypoplastic SMDGs with reduced numbers of convoluted tubules and a reduction in mucin immunolocalization (Blecher et al., 1983; Jaskoll et al., 2003). In contrast to this, the knockout mouse of the *Edar* receptor gene, known as *downless*, developed dysplastic SMDGs, showing a severe lack of ducts and acini, and virtually no detection of mucus (Jaskoll et al., 2003). Furthermore, addition of exogenous EDA protein addition to developing SMDGs in culture, as well as elevated expression of EDAR signalling in adult mice, gave rise to an increase in SMDG epithelial branches (Chang et al., 2009; Jaskoll et al., 2003). Addition of EDA protein to cultured *Eda* hemizygous (*Tabby)* SMDGs *in vitro* can also rescue branching in these mutant glands (Wells et al., 2010). Investigation of the minor salivary glands additionally emphasised the role of Eda signalling in gland branching morphogenesis as these glands of the tongue do not develop in *Tabby* and *downless* mice (Wells et al., 2011).

Analysis of the *Tabby* mouse in a classical study revealed that specific groups of the anterior nasal SMGs were completely absent while others developed normally (Grüneberg, 1971). It was reported that the Steno's gland and MSG develop in the *Tabby*, while some, but not all of the LNGs were completely absent (Grüneberg, 1971). Furthermore, all of the MNGs were reported missing (Grüneberg, 1971). Of the LNGs that did develop in the *Tabby*, these glands were described as rudimentary from the beginning, and their distal branched glands were also defective (Grüneberg, 1971). Defects in nasal glands have also been reported in HED patients, with patients suffering from dryness of the nasal mucosa, severe nasal crusting and foul smelling nasal discharge (Al-Jassim & Swift, 1996; Dietz et al., 2013).

Morphology and Development of the Tracheal SMGs

Developmental of the tracheal SMGs observed from animals models can be described in four distinct stages (Keswani et al., 2011; Thurlbeck et al., 1961). Stage 1 of development is the initial bud stage where an epithelium swelling is seen to immerge from the RE (**Error! Reference source not found.**, A). Stage 2 is characterised by the epithelial bud elongating into the underlying mesenchyme and cavitation occurs within this stalk to form a lumen (**Error! Reference source not found.**, B). This is followed by Stage 3 where canalized stalks begin to branch within the underlying mesenchyme (**Error! Reference source not found.**, C), while Stage 4 is classified as

the cellular differentiation stage, indicated by mucus production within the gland (**Error! Reference source not found.**, D). Unlike the nasal glands that develop for approximately two days as a long gland duct, followed by the branching of a distal gland the tracheal SMGs bud, elongate with a short stem, cavitate and begin branching. This developmental mechanism is similar to that seen in the branching of both the major and minor salivary glands, however in these structures branching occurs before lumen formation (Melnick & Jaskoll, 2000; Teshima et al., 2011).

In CD1 mice, the first signs of tracheal bud initiation can be identified adjacent to the cricoid cartilage in the ventral trachea at late E18.5. At P0 some ventral glands were observed at Stage 1 of budding, while others had extended and branched and had already begun Stage 3 of lumen formation and branching (Figure 10, C). At birth, some gland buds were also found in more dorsolateral planes, with a wave of initiation starting in the ventral regions and spreading more dorsally (Figure 10, D). Initiation before birth is earlier than previously described for the tracheal SMGs (Rawlins % Hogan, 2005) and may represent differences in genetic background (Borthwick et al., 1999; Innes & Dorin, 2001). Different inbred strains of mice show different posterior extensions of the SMGs between cartilage rings, while CFTR knockout mice have an increase in posterior extension with mutants showing glands as far as the eighth cartilage ring compared to the fourth ring in WT littermates (Borthwick et al., 1999; Innes & Dorin, 2001)

By P1, branching continues in both the ventral and dorsal glands, as well as continued induction of new buds throughout the dorsolateral walls. By P2, more newly forming SMGs arose in the anterior tracheal mesenchyme in dorsolateral positions (Figure 10, F), while ventral glands progressed to the branching and mucus producing (Figure 10, E). By P4, the ventral and dorsolateral glands continued to undergo extensive branching and cellular differentiation (Figure 10, G and H). The first signs of SMG formation in a posterior direction between the first and second cartilage rings was observed in the ventral trachea at approximately P4 (Figure 10, G). By P8, established anterior glands were continuing their branching as well as new glands appearing between C2 and C3 and progressively at P12 glands were found between C3 and C4 in ventral cross-sections. At P15 glands had developed between C4 and C5 and were producing mucus. During postnatal development, glands arose in a gradient from the ventral to dorsal areas of the trachea, in conjunction with their posterior development.

By P22, glands were well established and observed as posterior as C6 and initiation of new glands appeared to cease (Borthwick et al., 1999; Rawlins & Hogan, 2005).

Signalling During Tracheal SMG Development

To date, no investigation into the role of the canonical Wnt signalling pathway has been carried out on the tracheal SMGs. Similar to the nasal glands however, tracheal SMGs have been reported to be completely absent in the adult *Tabby* mouse, as well as in the early *crinkled* mice, the model of *Edaradd* mutation, at P7, indicating that EDA signalling is required for early SMG initiation and budding (Rawlins & Hogan, 2005). Complimentary to these findings, human patients with HED have been reported to have reduced numbers of seromucous respiratory glands, asthma like symptoms and respiratory tract infections (Callea et al. 2013). Furthermore, allergic response is increased in those with HED (Vanselow et al. 1970).

The bone morphogenetic proteins (BMPs) belong to the transforming growth factor β (TGFβ) superfamily (Miyazono et al., 2010). The BMPs play a multitude of roles during early embryonic patterning and morphogenesis such as the regulation of cell proliferation, differentiation, apoptosis and cell-fate determinations (Hogan, 1996; Kishigami & Mishina, 2005). Twenty BMPs have been identified, all having heterogeneous functions during developmental processes such as neurogenesis, bone and cartilage formation, and organogenesis (Hogan, 1996; Zhao, 2003).

In general, the BMP pathway involves the extracellular BMP ligands binding to the cell membrane bound BMP receptors (BMPR). These receptors are serine-threonine kinase receptors that belong to two groups, Type I and Type II (Massagué et al., 1994). BMPs bind to the Type I BMPR with higher affinity to that of Type II (Kirsch et al., 2000; Wrana et al., 1994). In order for ligand binding to stimulate an intracellular signal, heterodimerization of one Type I and one Type II BMPR is required. Upon BMP ligand binding to the Type I receptor, the Type II receptor is recruited (Carreira et al., 2014; Kirsch et al., 2000). The Type II BMPR then catalyses the phosphorylation of the intracellular serine-threonine domain of the Type 1 BMPR, recruiting a cytoplasmic receptor-activated Smad protein (either Smad1, 5 or 8). (Wrana et al., 1994). Phosphorylation of one of these Smads triggers the recruitment

of another cytoplasmic Smad, Smad4 (Whitman, 1998). This dimeric Smad complex can now translocate into the nucleus where BMP target genes can be activated. A number of extracellular antagonists also function in regulating the pathway. These include such soluble proteins as Noggin, Gremlin and Chordin, which form complexes with BMP ligands, preventing them from binding to their cell receptors (Walsh et al., 2010; Yanagita, 2005).

It has been previously shown that BMP signalling is critical for the development and patterning of the trachea and lungs (Eblaghie et al., 2006; Li et al., 2008; Weaver et al., 1999). During SMDG development, *Bmp4* is mesenchymally expressed and addition of BMP4 protein to developing SMDGs *in vitro* SMDG inhibits gland budding (Hoffman et al., 2002), indicating an antagonizing role in the control of the number of gland branches. Furthermore, when SMDGs are cultured with BMP antagonist sFRP1, branching of SMDGs is induced with a 26% increase observed in the amount of gland buds in treated glands compared to controls (Patel et al., 2011). In contrast BMP7 seems to enhance gland branching. In the *Bmp7* knockout mouse, a reduction in epithelial branches of the SMDG as well as disorganized mesenchyme surrounding the gland was observed (Jaskoll et al., 2002).

The only investigation into the roles of BMP signalling in respiratory gland development have been shown during that of the tracheal SMGs (Rawlins & Hogan, 2005). Using the *Bmp4*^{lacz} reporter mouse, it was reported that at P2 when tracheal buds were initiating from the RE, *Bmp4* was expressed throughout the underlying mesenchyme. During later development at P7, *Bmp4* detection was reduced and found only in the mesenchyme close to the newly formed gland branches (Rawlins & Hogan, 2005). By P28, *Bmp4* expression had reduced even further, and was only detected in a few mesenchymal cells (Rawlins & Hogan, 2005). The exact role of BMP4, or other BMPs, during respiratory gland development has not been elucidated.

Fibroblast growths factors (FGFs) make up one of the largest family of polypeptide proteins critical for tissue patterning and development of branching organs. Today, 22 members (FGF1-FGF22) of the FGF family are known within the human genome (Ornitz & Itoh, 2001). Four cell membrane-bound FGF receptors (FGFRs) have been identified in vertebrates, each having different affinities for different FGF ligands.

The four receptors, FGFR1-FGFR4, are composed of the common protein structure of most tyrosine kinase (TK) receptors (Johnson et al., 1990). The initiation of an intracellular signalling transduction pathway relies on extracellular binding of FGF ligands its target receptor, leading to receptor dimerization and intracellular phosphorylation of the TK domains of each receptor (Jiang & Hunter, 1999; Schlessinger, 1988). Following TK phosphorylation, a number of intracellular signalling cascades are triggered that are required for a multitude of developmental processes. These include the phospholipase C gamma (PLC-ϒ) pathway which initiates calcium release and activates protein kinase C to influence cell motility (Burgess et al., 1990; Mohammadi et al., 1991), and the phosphatidylinositol-3 kinase (PI3K) which activates Akt/protein kinase B needed for the mediation of cell survival (Ong et al., 2001). The most common route of FGF signalling during developmental processes is through the activation of the rat sarcoma homologue (RAS)/mitogen-activated protein kinase (MAPK) cascade. This pathway functions in activating target genes involved in cellular differentiation and proliferation.

The roles of a number FGFs have been shown to be critical for gland morphogenesis. *Fgf10* is expressed in the mesenchyme underlying the presumptive salivary gland epithelium from E11.5 (Wells et al., 2013). Jaskoll et al. (2005) showed in *Fgf10* null mice, as well as the *Fgfr2b* knockouts, that the SMDG initiated to the *Initial Bud* stage at E12.5 however it was unable to develop further, and at E13.5 any epithelial evidence of the SMDG was absent. Culture of SMDGs with FGF7 gave rise to moderate stalk extension and induced epithelial bud enlargement (Koyama et al., 2008). Inhibition of salivary gland branching by FGFR2b antisense oligonucleotides was also rescued by the addition of exogenous FGF7 which stimulated cell proliferation and end bud formation (Steinberg et al., 2005). Using *Fgf8* hypomorphic embryos, as well as *Fgf8* conditional knockout mutants, it has also been described that SMDG bud initiation is independent of *Fgf8*, however expression is required for continued SMDG branching morphogenesis and survival (Jaskoll et al., 2004a). At approximately E13.5 when the lacrimal gland bud arises on the temporal side of the eye, *Fgf10* expression is seen in the periocular mesenchyme adjacent to the budding gland and distal to the tip of the gland as it is elongating at E14.5 (Makarenkova et al., 2000). Investigation of *Fgf10 -/-* mice at E18.5 also showed the complete absence of the lacrimal gland (Makarenkova et al., 2000). While *Fgf7* expression was not as

evident as that of *Fgf10* in the periocular mesenchyme during normal *in vivo* lacrimal gland development, application of an FGF7 bead to lacrimal gland explant cultures induced ectopic gland bud formation, similarly to FGF10 protein application, however not at as high a rate (Makarenkova et al., 2000). The respiratory gland phenotype has not been investigated in any *Fgf* homozygous knockout mice, however, Rawlins and Hogan (2005) established that in *Fgf10* heterozygous mice at P20 fewer tracheal SMGs developed. Of the glands that did develop, they were only located anteriorly by the CC and C1 and had not undergone full branching while no glands were seen between the more posterior cartilaginous rings (Rawlins & Hogan, 2005). The role of FGF signalling during nasal and tracheal SMG development has not been investigated. It has also been shown that tracheal cartilage ring defects occur in *Fgf10* homozygous mice, which may also have a secondary affect on tracheal SMG development (Sala et al., 2011). It is therefore possible that in addition to a direct defect of FGFs on gland elongation and branching, a tracheal ring defect might compromise the arrangement of the tracheal SMG development.

Future Directions

In this review we describe a detailed account of anterior nasal and tracheal SMG development. We highlight that the SMGs show distinct morphological stages of development, beginning with bud formation, followed by duct elongation, distal gland branching and acinar differentiation (Table 1). Now that the morphology of these glands has been elucidated, further research into the mechanisms involved in their budding and arborisation is encouraged. As we report here, studies have looked at early bud induction of the nasal glands, and the roles played by the canonical Wnt signalling pathway (Driskell et al., 2007; Duan et al., 1999) (Figure 11). The involvement of Wnt activity during later duct elongation and distal gland branching stages of the nasal SMGs is however unknown. In addition, the role of Wnt signalling during tracheal SMG development has not been analysed (Figure 11). Requirement for Ectodysplasin A signalling has been emphasised by the absence of some nasal and all tracheal SMGs in the *Tabby* mutant (Grüneberg, 1971; Rawlins & Hogan, 2005) (Figure 11). In keeping with this mouse data, human patients of HED also develop airway obstruction and pulmonary infection (Dietz et al., 2013). The nasal gland phenotype observed in the *Tabby* mouse indicates that different subsets of nasal SMGs utilise different cues, with the Steno's gland and the MSG developing normally

in the absence of Eda signalling, while the medial nasal glands are completely absent (Grüneberg 1971). Thus glands with similar morphology may develop using different signalling pathways. This is also emphasised by the difference in lumen formation used to create a final hollow duct. The Steno's gland develops with a preformed lumen, similar to the lung, while the other LNGs and MNGs develop as solid cords of cells that are cavitated at later stages to create a lumen, similar to salivary glands (Figure 11). Thus there are different mechanisms at play to form anatomically similar structures. Further down the respiratory tree, participation of *Fgf10* during trachea SMG development has been shown to be essential for successful gland branching morphogenesis (Rawlins & Hogan, 2005) (Figure 11). Analysis of the role of *Fgf10* during nasal SMG development, or its requirement for early tracheal SMG bud initiation has not been explained however. Furthermore, while previous studies have hinted at roles played by the signalling factors mentioned above, other developmentally important pathways during SMG organogenesis have not been touched upon. For example, Sonic hedgehog (Shh) expression is localised to ducts and terminal end buds of the developing SMDG (Jaskoll et al. 2004b). In the *Shh -/-* mouse at E18.5, an undifferentiated dysplastic gland forms, suggesting that during SMDG development *Shh* is required for gland growth and cellular differentiation (Jaskoll et al. 2004b). Interestingly, mammary gland branching morphogenesis is independent of SHH signalling, as glands in the *Shh -/-* mouse are indistinguishable of those observed in wild type littermates (Michno et al., 2003). This data collectively poses interesting questions for the role and regulatory functions of *Shh* in SMG development. Additionally, epidermal growth factors (EGFs) have been described to be essential for successful development of both SMDGs and mammary glands (Kashimata et al., 2000; Luetteke et al., 1999), however this pathway has not been studied in any of the respiratory SMGs. To this end, continual investigation is imperative to delineate the cellular mechanisms and intracellular cues that are required for successful SMG morphogenesis. This will provide insight into how development of SMGs influences function, and thus help clarify their role in pulmonary diseases.

Acknowledgements

We would like to thank the Dental Institute of King's College London for funding this work.

References

Aikawa T., Shimura S., Sasaki H., Ebina M., Takishima T. 1992. Marked goblet cell hyperplasia with mucus accumulation in the airways of patients who died of severe acute asthma attack. Chest 101: 916–921.

Al-Jassim A.H., Swift A.C. 1996. Persistent nasal crusting due to hypohidrotic ectodermal dysplasia. J. Laryngol. Otol. 110: 379-382.

Arce L., Yokoyama N.N., Waterman M.L. 2006. Diversity of LEF/TCF action in development and disease. Oncogene 25: 7492–7504.

Ballard S.T., Spadafora D. 2007. Fluid secretion by submucosal glands of the tracheobronchial airways. Respir. Physiol. Neurobiol. 159: 271–277.

Basbaum C., Jany B., Finkbeiner W. 1990. The Serous Cell. Annu. Rev. Physiol. 52: 97–113.

Blecher S.R., Debertin M., Murphy J.S. 1983. Pleiotropic effect of Tabby gene on epidermal growth factor-containing cells of mouse submandibular gland. Anat. Rec. 207: 25–29.

Bojsen-Moller F. 1964. Topography of the nasal glands in rats and some other mammals. Anat. Rec. 150: 11–24.

Bojsen-Moller F. 1967. Topography and development of anterior nasal glands in pigs. J. Anat. 101: 321–331.

Borthwick D.W., West J.D., Keighren M. A., Flockhart J.H., Innes B. A., Dorin J.R. 1999. Murine submucosal glands are clonally derived and show a cystic fibrosis gene-dependent distribution pattern. Am. J. Respir. Cell Mol. Biol. 20: 1181–1189.

Broman I. 1921. Über die Entwicklung der konstanten grösseren Nasennebenhöhlendrüsen der Nagetiere. Z. Anat. Entwickl. Gesch. 60: 439–586.

Brunner H. 1942. Nasal Glands. Arch. Otolaryngol. 35: 183–209.

Burgess W., Dionne C., Kaplow J., Mudd R., Friesel R., Zilberstein A., Schlessinger J., Jaye M. 1990. Characterization and cDNA Cloning of Phospholipase C--y , a Major Substrate for Heparin-Binding Growth Factor 1 (Acidic Fibroblast Growth Factor)-Activated Tyrosine Kinase. Mol. Cell. Biol. 10: 4770–4777.

Butler D.G. 2002. Hypertonic fluids are secreted by medial and lateral segments in duck (Anas platyrhynchos) nasal salt glands. J. Physiol. 540: 1039–1046.

Carreira A. C., Lojudice F.H., Halcsik E., Navarro R.D., Sogayar M.C., Granjeiro J.M. 2014. Bone morphogenetic proteins: facts, challenges, and future perspectives. J. Dent. Res. 93: 335–345.

Chang S.H., Jobling S., Brennan K., Headon D.J. 2009. Enhanced Edar signalling has pleiotropic effects on craniofacial and cutaneous glands. PLoS One 4: e7591.

Clarke A., Phillips D.I., Brown R., Harper P.S. 1987. Clinical aspects of X-linked hypohidrotic ectodermal dysplasia. Arch. Dis. Child. 62: 989–996.

Cuschieri A., Bannister L.H. 1974. Some histochemical observations on the mucosubstances of the nasal glands in the mouse. Histochem. J. 6: 543–558.

Davidson G., Wu W., Shen J., Bilic J., Fenger U., Stannek P., Glinka A., Niehrs C. 2005. Casein kinase 1 gamma couples Wnt receptor activation to cytoplasmic signal transduction. Nature 438: 867–872.

Dean C.H., Miller L.A.D., Smith A.N., Dufort D., Lang R. A., Niswander L.A. 2005. Canonical Wnt signaling negatively regulates branching morphogenesis of the lung and lacrimal gland. Dev. Biol. 286: 270–86.

Dietz J., Kaercher T., Schneider A.T., Zimmermann T., Huttner K., Johnson R., Schneider H. 2013. Early respiratory and ocular involvement in X-linked hypohidrotic ectodermal dysplasia. Eur. J. Pediatr. 172: 1023–1031.

Döffinger R., Smahi A., Bessia C., Geissmann F., Feinberg J., Durandy A, Bodemer C., Kenwrick S., Dupuis-Girod S., Blanche S., Wood P., Rabia S.H., Headon D.J., Overbeek P.A, Le Deist F., Holland S.M., Belani K., Kumararatne D.S., Fischer A., Shapiro R., Conley M.E., Reimund E., Kalhoff H., Abinun M., Munnich A., Israël A., Courtois G., Casanova J.L. 2001. X-linked anhidrotic ectodermal dysplasia with immunodeficiency is caused by impaired NF-kappaB signaling. Nat. Genet. 27: 277–85.

Driskell R.R., Goodheart M., Neff T., Liu X., Luo M., Moothart C., Sigmund C.D., Hosokawa R., Chai Y., Engelhardt J.F. 2007. Wnt3a regulates Lef-1 expression during airway submucosal gland morphogenesis. Dev. Biol. 305: 90–102.

Driskell R.R., Liu X., Luo M., Filali M., Zhou W., Abbott D., Cheng N., Moothart C., Sigmund C.D., Engelhardt J.F. 2004. Wnt-responsive element controls Lef-1 promoter expression during submucosal gland morphogenesis. Am. J. Physiol. Lung Cell. Mol. Physiol. 287: L752–763.

Duan D., Sehgal A, Yao J., Engelhardt J.F. 1998. Lef1 transcription factor expression defines airway progenitor cell targets for in utero gene therapy of submucosal gland in cystic fibrosis. Am. J. Respir. Cell Mol. Biol. 18: 750–758.

Duan D., Yue Y., Zhou W., Labed B., Ritchie T.C., Grosschedl R., Engelhardt J.F. 1999. Submucosal gland development in the airway is controlled by lymphoid enhancer binding factor 1 (LEF1). Development 126: 4441–4453.

Eastman Q., Grosschedl R. 1999. Regulation of LEF-1/TCF transcription factors by Wnt and other signals. Curr. Opin. Cell Biol. 11: 233–240.

Eblaghie M.C., Reedy M., Oliver T., Mishina Y., Hogan B.L.M. 2006. Evidence that autocrine signaling through Bmpr1a regulates the proliferation, survival and morphogenetic behavior of distal lung epithelial cells. Dev. Biol. 291: 67–82.

Engelhardt J.F., Yankaskas J.R., Ernst S.A., Yang Y., Marino C.R., Boucher R.C., Cohn J.A., Wilson J.M. 1992. Submucosal glands are the predominant site of CFTR expression in the human bronchus. Nat. Genet. 2: 240–248.

Finkbeiner W.E. 1999. Physiology and pathology of tracheobronchial glands. Respir. Physiol. 118: 77–83.

Freeman J. A. 1962. Fine structure of the goblet cell mucous secretory process. Anat. Rec. 144: 341–357.

Frisch D. 1967. Ultrastructure of the mouse olfactory mucosa. Am. J. Anat. 121: 87–120.

Getchell M.L., Getchell T. V. 1992. Fine structural aspects of secretion and extrinsic innervation in the olfactory mucosa. Microsc. Res. Tech. 23: 111–127.

Gilmore T.D. 2006. Introduction to NF-kappaB: players, pathways, perspectives. Oncogene 25: 6680–6684.

Gross E. A, Swenberg J. A, Fields S., Popp J. A. 1982. Comparative morphometry of the nasal cavity in rats and mice. J. Anat. 135: 83–88.

Grüneberg H. 1971. The glandular aspects of the tabby syndrome in the mouse. J. Embryol. Exp. Morphol. 25: 1–19.

Hai B., Yang Z., Millar S.E., Choi Y.S., Taketo M.M., Nagy A., Liu F. 2010. Wnt/B-Catenin Signaling Regulates Postnatal Development and Regeneration of the Salivary Gland. Stem Cells Dev. 19: 1793–1801.

He X., Semenov M., Tamai K., Zeng X. 2004. LDL receptor-related proteins 5 and 6 in Wnt/beta-catenin signaling: arrows point the way. Development 131, 1663–1677.

Headon D.J., Overbeek P. A. 1999. Involvement of a novel Tnf receptor homologue in hair follicle induction. Nat. Genet. 22: 370–374.

Hoffman M., Kidder B., Steinberg Z., Lakhani S., Ho S., Kleinman H., Larsen M. 2002. Gene expression profiles of mouse submandibular gland development: FGFR1 regulates branching morphogenesis in vitro through BMP- and FGF-dependent mechanisms. Development 129: 5767–5778.

Hogan B.L. 1996. Bone morphogenetic proteins: multifunctional regulators of vertebrate development. Genes Dev. 10: 1580–1594.

Innes B. A., Dorin J.R. 2001. Submucosal gland distribution in the mouse has a genetic determination localized on Chromosome 9. Mamm. Genome 12: 124–128.

Jacob A., Chole R. A. 2006. Survey anatomy of the paranasal sinuses in the normal mouse. Laryngoscope 116: 558–563.

Jaskoll T., Abichaker G., Witcher D., Sala F.G., Bellusci S., Hajihosseini M.K., Melnick M. 2005. FGF10/FGFR2b signaling plays essential roles during in vivo embryonic submandibular salivary gland morphogenesis. BMC Dev. Biol. 5: 11.

Jaskoll T., Leo T., Witcher D., Ormestad M., Astorga J., Bringas P. Jr, Carlsson P., Melnick M. 2004b. Sonic Hedgehog Signaling Plays an Essential Role During Embryonic Salivary Gland Epithelial Branching Morphogenesis. Dev. Dyn. 229: 722–732.

Jaskoll T., Witcher D., Toreno L., Bringas P., Moon A.M., Melnick M. 2004a. FGF8 dose-dependent regulation of embryonic submandibular salivary gland morphogenesis. Dev. Biol. 268: 457–469.

Jaskoll T., Zhou Y., Chai Y., Makarenkova H., Collinson J., West J., Hajihosseini M., Lee J., Melnick M. 2002. Embryonic Submandibular Gland Morphogenesis: Stage-Specific Protein Localization of FGFs, BMPs ,Pax6 and Pax9 in Normal Mice and Abnormal SMG Phenotypes in FgfR2-IIIc +/c+delta, BMP7 –/– and Pax6 –/– Mice. Cells Tissues Organs 170: 83–98.

Jaskoll T., Zhou Y.M., Trump G., Melnick M. 2003. Ectodysplasin receptor-mediated signaling is essential for embryonic submandibular salivary gland development. Anat Rec A Discov Mol Cell Evol Biol 271: 322–331.

Jiang G., Hunter T. 1999. Receptor Signalling: When dimerization is not enough. Curr. Biol. 9: R568–571.

Johnson D.E., Lee P.L., Lu J., Williams L.T. 1990. Diverse Forms of a Receptor for Acidic and Basic Fibroblast Growth Factors. Mol. Cell. Biol. 10: 4728–4736.

Kashimata M., Sayeed S., Ka A., Onetti-Muda A., Sakagami H., Faraggiana T., Gresik E.W. 2000. The ERK-1/2 signaling pathway is involved in the stimulation of branching morphogenesis of fetal mouse submandibular glands by EGF. Dev. Biol. 220: 183–196.

Kerjaschki D. 1974. The anterior medial gland in the mouse nasal septum: an uncommon type of epithelium with abundant innervation. J. Ultrastruct. Res. 46: 466–482.

Keswani S.G., Le L.D., Morris L.M., Lim F.Y., Katz A.B., Ghobril N., Habli M., Frischer J.S., Crombleholme T.M. 2011. Submucosal gland development in the human fetal trachea xenograft model: implications for fetal gene therapy. J. Pediatr. Surg. 46: 33–38.

Kirsch T., Sebald W., Dreyer M. 2000. Crystal structure of the BMP-2 – BRIA ectodomain complex. Nat. Struct. Mol. Biol. 7: 492–496.

Kishigami S., Mishina Y. 2005. BMP signaling and early embryonic patterning. Cytokine Growth Factor Rev. 16: 265–278.

Klockars M., Reitamo S. 1975. Tissue Distribution of Lysozyme in Man. J. Histochem. Cytochem. 23: 932-940

Komiya Y., Habas R. 2008. Wnt signal transduction pathways. Organogenesis. 4: 68–75.

Koyama N., Hayashi T., Ohno K., Siu L., Gresik E.W., Kashimata M. 2008. Signaling pathways activated by epidermal growth factor receptor or fibroblast growth factor receptor differentially regulate branching morphogenesis in fetal mouse submandibular glands. Dev. Growth Differ. 50: 565–576.

Li Y., Gordon J., Manley N. 2008. Bmp4 is required for tracheal formation: a novel mouse model for tracheal agenesis. Dev. Biol. 322: 145–155.

Liu C., Li Y., Semenov M., Han C., Baeg G.H., Tan Y., Zhang Z., Lin X., He X. 2002. Control of beta-catenin phosphorylation/degradation by a dual-kinase mechanism. Cell 108: 837–847.

Luetteke N.C., Qiu T.H., Fenton S.E., Troyer K.L., Riedel R.F., Chang, A., Lee, D.C. 1999. Targeted inactivation of the EGF and amphiregulin genes reveals distinct roles for EGF receptor ligands in mouse mammary gland development. Development 126: 2739–2750.

Makarenkova H.P., Ito M., Govindarajan V., Faber S.C., Sun L., McMahon G., Overbeek P.A, Lang R.A. 2000. FGF10 is an inducer and Pax6 a competence factor for lacrimal gland development. Development 127: 2563–2572.

Massagué J., Attisano L., Wrana J.L. 1994. The TGF-β family and its composite receptors. Trends Cell Biol. 4: 172-178

Masson P.L., Heremans J.F., Prignot J.J., Wauters G. 1966. Immunohistochemical localization and bacteriostatic properties of an iron-binding protein from bronchial mucus. Thorax 21:538–44.

Melnick M., Jaskoll T. 2000. Mouse Submandibular Gland Morphogenesis: a Paradigm for Embryonic Signal Processing. Crit. Rev. Oral Biol. Med. 11: 199–215.

Meyrick B., Reid L. 1970. Ultrastructure of cells in the human bronchial submucosal glands. J. Anat. 107: 281–299.

Meyrick B., Sturgess J.M. Reid L., 1969. A reconstruction of the duct system and secretory tubules of the human bronchial submucosal gland. Thorax 24: 729–736.

Michno K., Boras-Granic K., Mill P., Hui C., Hamel P.A. 2003. Shh expression is required for embryonic hair follicle but not mammary gland development. Dev. Biol. 264: 153–165.

Mikkola M.L. 2009. Molecular aspects of hypohidrotic ectodermal dysplasia. Am. J. Med. Genet. A. 149A: 2031–2036.

Miyazono K., Kamiya Y., Morikawa M. 2010. Bone morphogenetic protein receptors and signal transduction. J. Biochem. 147: 35–51.

Moe H., Bojsen-Moller F. 1971. The Fine Structure of the Lateral Nasal Gland (Steno's Gland) of the Rat. J. Ultrastruct. Res. 36: 127–148.

Mohammadi M., Honegger A., Rotin D., Fischer R., Bellot F., Li W., Dionne C., Jaye M., Rubenstein M., Schlessinger J. 1991. A tyrosine-phosphorylated carboxy-terminal peptide of the fibroblast growth factor receptor (Flg) is a binding site for the SH2 domain of phospholipase C--yl. Mol. Cell. Biol. 11: 5068–5078.

Morlon A., Munnich A., Smahi A. 2005. TAB2, TRAF6 and TAK1 are involved in NF-kappaB activation induced by the TNF-receptor, Edar and its adaptator Edaradd. Hum. Mol. Genet. 14: 3751–3757.

Oeckinghaus A., Ghosh S. 2009. The NF-kappaB family of transcription factors and its regulation. Cold Spring Harb. Perspect. Biol. 1: a000034.

Ong S.H., Hadari Y.R., Gotoh N., Guy G.R., Schlessinger J., Lax I. 2001. Stimulation of phosphatidylinositol 3-kinase by fibroblast growth factor receptors is mediated by coordinated recruitment. PNAS 98: 6074–6079.

Oppenheimer E., Esterly J. 1975. Pathology of cystic fibrosis: review of the literature and comparison with 146 autopsied cases. In Perspectives in Pediatric Pathology, (Eds. H. Rosenberg, R. Bolande), pp. 241-278. Yearbook Medical Publishers, Chicago, USA.

Ornitz D., Itoh N. 2001. Fibroblast growth factors. Genome Biol. 2: 1–12.

Ornoy A., Arnon J., Katznelson D., Granat M., Caspi B., Chemke J. 1987. Pathological confirmation of cystic fibrosis in the fetus following prenatal diagnosis. Am. J. Med. Genet. 28: 935–947.

Patel N., Sharpe P.T., Miletich I. 2011. Coordination of epithelial branching and salivary gland lumen formation by Wnt and FGF signals. Dev. Biol. 358: 156–167.

Phillips J.E., Ji L., Rivelli M.A, Chapman R.W., Corboz M.R. 2009. Three-dimensional analysis of rodent paranasal sinus cavities from X-ray computed tomography (CT) scans. Can. J. Vet. Res. 73: 205–211.

Popp J., Martin J. 1984. Surface Topography and Distribution of Cell Types in the Rat Nasal Respiratory Epithelium: Scanning Electron Microscopic Observations. Am. J. Anat. 436: 425–436.

Purves D., Augustine G.J., Fitzpatrick D., Katz L.C., LaMantia A.S., McNamara J.O., Williams. S.M. 2004. The Olfactory Epithelium and Olfactory Receptor Neurons. In: Neuroscience. pp. 337–370. Sinauer Associates, Inc., Sunderland, MA.

Rawlins E.L., Hogan B.L.M. 2005. Intercellular growth factor signaling and the development of mouse tracheal submucosal glands. Dev. Dyn. 233: 1378–1385.

Reid L. 1960. Measurement of the bronchial mucous gland layer: a diagnostic yardstick in chronic bronchitis. Thorax 15: 132–41.

Rogers D.F. 2004. Airway mucus hypersecretion in asthma: an undervalued pathology? Curr. Opin. Pharmacol. 4: 241–250.

Rogers D.F. 2008. Airway Mucus Hypersecretion in Asthma and COPD: Not the Same? In Asthma and COPD. Basic Mechanisms and Clinical Management, (Eds. P. Barnes, J. Drazen, S. Rennard, N. Thomson), pp. 211-223. Academic Press Inc.

Sala F.G. Del Moral P.M., Tiozzo C., Alam D.A, Warburton D., Grikscheit T., Veltmaat J.M., Bellusci S., 2011. FGF10 controls the patterning of the tracheal cartilage rings via Shh. Development 138: 273–282.

Schlessinger J. 1988. Signal transduction by allosteric receptor oligomerization. Trends Biochem. Sci. 13: 443–447.

Srivastava A., Pispa J., Hartung A., Du Y., Ezer S., Jenks T., Shimada T., Pekkanen M., Mikkola M.L., Ko M.S., Thesleff I., Kere J., Schlessinger D. 1997. The Tabby phenotype is caused by mutation in a mouse homologue of the EDA gene that reveals novel mouse and human exons and encodes a protein (ectodysplasin-A) with collagenous domains. Proc. Natl. Acad. Sci. U. S. A. 94: 13069–13074.

Steinberg Z., Myers C., Heim V.M., Lathrop C. A, Rebustini I.T., Stewart J.S., Larsen M., Hoffman M.P. 2005. FGFR2b signaling regulates ex vivo submandibular gland epithelial cell proliferation and branching morphogenesis. Development 132: 1223–1234.

Sturgess J., Imrie J. 1982. Quantitative evaluation of the development of tracheal submucosal glands in infants with cystic fibrosis and control infants. Am. J. Pathol. 106: 303–311.

Teshima T.H.N., Ianez R.F., Coutinho-Camillo C.M., Buim M.E., Soares F. A, Lourenço S. V. 2011. Development of human minor salivary glands: expression of mucins according to stage of morphogenesis. J. Anat. 219: 410–417.

Thurlbeck W., Benjamin B., Reid L. 1961. Development and distribution of mucous glands in the foetal human trachea. Br. J. Dis. Chest 55: 54–64.

Van Genderen C., Okamura R.M., Farinas I., Quo R.G., Parslow T.G., Bruhn L., Grosschedl R. 1994. Development of several organs that require inductive epithelial-mesenchymal interactions is impaired in LEF-1-deficient mice. Genes Dev. 8: 2691–2703.

Vidić B. 1971. The prenatal morphogenesis of the lateral nasal wall in the rat (Mus rattus). J. Morphol. 133: 303–17.

Vidić B., Greditzer H.G. 1971. The histochemical and microscopical differentiation of the respiratory glands around the maxillary sinus of the rat. Am. J. Anat. 132: 491–513.

Walsh D.W., Godson C., Brazil D.P., Martin F. 2010. Extracellular BMP-antagonist regulation in development and disease: tied up in knots. Trends Cell Biol. 20: 244–56.

Weaver M., Yingling J.M., Dunn N.R., Bellusci S., Hogan B.L.M. 1999. Bmp signaling regulates proximal-distal differentiation of endoderm in mouse lung development. Development 126: 4005–4015.

Wells, K.L., Gaete, M., Matalova, E., Deutsch, D., Rice, D., Tucker, A.S. 2013. Dynamic relationship of the epithelium and mesenchyme during salivary gland initiation: the role of Fgf10. Biol. Open 2: 81–989.

Wells K.L., Mou C., Headon D.J., Tucker A.S. 2010. Recombinant EDA or sonic hedgehog rescue the branching defect in ectodysplasin a pathway mutant salivary glands in vitro. Dev. Dyn. 239: 2674–2684.

Wells K.L., Mou C., Headon D.J., Tucker A.S. 2011. Defects and rescue of the minor salivary glands in Eda pathway mutants. Dev. Biol. 349: 137–146.

Wells U., Widdicombe J.G. 1986. Lateral nasal gland secretion in the anaesthetized dog. J. Physiol. 374: 359–374.

Whitman M. 1998. Smads and early developmental signaling by the TGFbeta superfamily. Genes Dev. 12: 2445–2462.

Wine J.J., Joo N.S. 2004. Submucosal glands and airway defense. Proc. Am. Thorac. Soc. 1: 47–53.

Wrana J., Attisano L., Wieser R., Ventura F., Massague J. 1994. Mechanism of activation of the TGF-β receptor. Nature 370: 341–347.

Yanagita M. 2005. BMP antagonists: their roles in development and involvement in pathophysiology. Cytokine Growth Factor Rev. 16: 309–317.

Zeng X., Tamai K., Doble B., Li S., Huang H., Habas R., Okamura H., Woodgett J., He X. 2005. A dual-kinase mechanism for Wnt co-receptor phosphorylation and activation. Nature 438: 873–877.

Zhao G.Q. 2003. Consequences of knocking out BMP signaling in the mouse. Genesis 35: 43–56.

Figure Legends

Figure 1. Schematic illustration outlining the cellular composition of the treacheobronchial SMGs.

The tracheal glands are composed of sacs of serous cells, which form acini. Serous cells secrete a watery like secretion rich in bactericidal enzymes. Acini run into tubules of mucous cells, which secrete a thicker gel like substance rich in glycosylated proteins. These two types of secretions are then combined in a collecting duct, whose wall is composed of non-ciliated columnar epithelial cells. The collecting duct runs into a ciliated duct made of more respiratory epithelial-like cells that possess beating cilia on their apical surfaces. Mucus is secreted through this ciliated duct into the airway lumen where it covers the surface epithelium.

Figure 2. Anatomy of the nose and paranasal sinuses in humans.

(A) Sagittal view of the three distinct areas of the nose; vestibule, respiratory and olfactory regions. **(B)** Sagittal view of the lateral wall showing the curved concha and the inter-conchal meatuses. **(C)** Frontal section through the nasal chamber showing the position of the medial walls (yellow) on either side of the septum (S). Image shows the location of the superior concha (SC), the medial concha (MC) and the inferior concha (IC) of the lateral wall (orange) and their underlying meatuses. The frontal image also delineates the location the paranasal sinuses. SM=superior meatus; MM=middle meatus; IM=inferior meatus; FS=frontal sinus; ES=ethmoidal sinus; MS=maxillary sinus. Dotted black lines indicate opening of sinuses into nasal cavity found at a more caudal plane.

Figure 3. Steno's duct elongation and branching morphogenesis.

(A-D) The epithelial budding of the Steno's duct is seen between E12.0 and E12.5 from the REA. **(E-H)** By E13.5, the Steno's duct elongates over the nasal cavity and caudally extends through the mesenchyme of the medial concha. **(I-L)** By E14.5 the distal tip of the Steno's duct has reached the mesenchyme beneath the maxillary sinus to the location of where the Steno's gland will branch (J, red bracket). **(M-N)** The Steno's gland begins to branch from the Steno's duct between E15.0 and E15.5. The first signs of end buds are seen at E15.5. **(O-P)** By E17.5 the Steno's gland is continually branching and acinus differentiation is well established with most acinar

cells producing mucus (blue arrows). Maxillary sinus cavity (MS); Steno's gland (yellow arrows and dotted line); Division of RE to OE shown by pink arrows. C,G,K scale bar= 300μm, D,H,L scale bar = 500Mμm, M & O scale bar = 500μm; N & P scale bar = 250μm.

Figure 4. Budding locations of the LNGs from the protruding lip of the middle concha.

The LNG2 bud is first seen at E13.5 arising from the REP at the most rostral area of the conchal lip. It will extend caudally though the middle concha as development continues. At E14.5, LNG3 arises from the anterior area of the lip, underneath the opening of the Steno's duct through the REA, and will extend caudally adjacent to the duct of LNG2. At E15.5, LNG4 initiates below the origin of the LNG2 and extends posteriorly through the mesenchyme of the concha where it will eventually branch beneath the nasal cartilage capsule, anterior to the palatal shelf. LNG5 also initiates at E15.5, where it will elongate adjacent to the ducts of LNG2 and LNG3. Gland buds (2-5) shown in green, direction of future extending duct shown by red arrows. Schematic is taken at a sagittal view. Axis describes anterior (A), posterior (P), rostral (R) and caudal (C).

Figure 5. LNG duct elongation.

(A) Sagittal (S) and horizontal (H) planes through an E13.5 mouse head showing the location of the LNG2 bud. **(B)** Horizontal representation of LNG2 budding from the middle conchal lip. **(C)** Sagittal histological section showing the location of the middle conchal lip and the LNG2 bud in the nasal region. **(D)** The epithelial bud of LNG2 at E13.5. **(E-F)** Schematics showing location and appearance of the elongated LNG2 and the budding LNG3-5 at E14.5. **(G-H)** At E14.5 the LNG2 has elongated caudally as a solid stem. LNG3 has budded and begun to elongate and LNG4 is seen at a slightly earlier budding stage. **(I-J)** LNG5 is at its initial bud formation stage at E14.5. **(K)** Schematic showing the progression of the LNGs by E15.5. **(L-M)** A sagittal section shows the distal tips of LNG2 and LNG3 ending within the mesenchyme above the branching Steno's gland (yellow). The distal tip of LNG5 is found at a more rostral location adjacent to these ducts (shown in K). **(N-O)** LNG4 has elongated posteriorly with its distal tip emerging below the nasal cartilage

capsule. Left column of sagittal sections scale bar = 500μm; right column scale bar = 100μm.

Figure 6. Branching morphogenesis of the LNGs.

At E16.5 the LNGs begin branching of their distal glands. **(A-B)** LNG2 is the first to undergo branching between E15.5 and E16.5. At E16.5 many end buds are apparent and cavitation has begun within the gland acini (**B** - white arrows). LNG3 has also begun to branch at E16.5 as seen by the appearance of end buds (**B** – green arrows). **(C-D)** At E17.5, LNG2 and LNG3 have branched and formed distinctive acini with lumens. (**E-F**) At E16.5 the onset of branching of the LNG4 beneath the nasal capsule is evident (**F** – green arrows). (**G-H**) By E17.5, LNG4 has formed branches and end buds, and lumen formation has begun within acini (**H** – white arrows). (**I-J**) LNG5 is seen close to the ducts of LNG2 and LNG3, whit possible lumen formation beginning. A clear lumen is seen in the ducts of LNG2 and LNG3 at this stage (**J** – white arrows). (**K-**L) By E17.5, LNG5 has begun to branch with a clear lumen seen within its duct and lumen formation at its initial stages within acini. Left column of each age scale bar = 500μm; right column scale bar = 250μm.

Figure 7. MNG development.

(**A-D)** The development of the MNGs begins between E14.0-E14.5 with the budding and elongation of the ducts of MNG1 and MNG2. (**E-H**) The MNG1 and MNG2 ducts elongate to the central septal area by E15.5 and branching has initiated at the distal tip of MNG1 (inset image **H**). MNG3 has also budded and elongated, with its distal end adjacent to the midline of the MNG1 and MNG2 ducts (**E-F**). (**I-J**) Branching of MNG1 has progressed by E16.5 with an array of branches and terminal end buds apparent at this stage. MNG2 has also begun branching. The distal tip of MNG3 has extended close the branching ends of the other MNGs. (**K-L**) By E17.5, branching continues in all the MNGs in the central region of the septum. MNG4 has emerged by E17.5 as an elongated duct and the onset of branching has begun. Image A scale bar = 500μm; image B scale bar = 250μm.

Figure 8. MSG development.

The maxillary sinus gland initiates between E14.5 and E15.5. (**A-B**) No MSG primordium is evident at E14.5. (**C-D**) At E15.5 the MSG is seen to have invaginated

and branched into the mesenchyme close to its opening in the RE. The MSG continues to branch and grow at E16.5 (**E-F**) and E17.5 (**G-H**). MSG = red, Steno's gland = yellow, LNG2 = green. MS = maxillary sinus cavity. Image A scale bar = 500μm; Image B scale bar = 250μm.

Figure 9. Stages of tracheal SMG development

(A) Stage 1: Tracheal SMG buds are first seen to invaginate from the RE into the underlying mesenchyme. (B) Stage 2: Elongation of the bud and cavitation of the epithelial stalk occurs. (C) Stage 3: Epithelial stalk undergoes clefting and branching (D) Stage 4: Cellular differentiation is observed indicated by mucus staining within the glands by Alcian Blue. AL= airway lumen, L= lumen, M= mucus. Scale bar = 25μm.

Figure 10. Normal postnatal tracheal SMG development.

(A-B) Schematic representations of the ventral (A) and more dorsal (B) tissue sections cut through postnatal tracheal tissue. (C) Glands are seen to have reached the lumen formation stage in the ventral trachea by P0, while more dorsally they are seen at the branching stage (D). (E) At P2 ventral glands have continued to branch and cellular differentiation is indicated by mucus staining within gland lumens. Continued budding of new glands is seen in more anterior dorsal positions (F). (G-H) By P4 glands have branched extensively in the ventral mesenchyme as well as in the dorsal trachea. Glands are also seen at the branching stage between C1 and C2 in the ventral trachea (G). CC=cricoid cartilage, C1=first cartilage ring, C2=second cartilage ring etc. Black arrow = developing gland, green arrow = lumen formation, blue arrow = mucus production. Scale bar=100μm.

Figure 11. Possible paracrine factors required for early respiratory gland development.

(A) Steno's gland bud induction does not require EDA signalling, however the roles of other developmental molecules such as FGFs, BMPs, and WNTs have not been investigated during Steno's gland development. (B) The medial nasal glands have been reported to be absent in the *Tabby* mouse, indicating EDA signalling is imperative for their development. *Lef-1* expression has also been described in early nasal gland buds, indicating the involvement of WNT signalling. Requirement for

FGF or BMP signalling has not been investigated in the medial nasal glands. (C) Tracheal SMG investigation has shown the expression of *Edar* in the tracheal RE, and the absence of tracheal SMGs in the *Tabby* mouse, emphasising the role of EDA signalling during SMG bud induction. Branching morphogenesis of tracheal SMGs is also reduced in *Fgf10* +/- adult mouse, indicating its need for successful development. While *Bmp4* is expressed surrounding development tracheal SMGs, the exact role of this molecule or the BMP pathway has not been investigated. Finally, WNT signalling has not been analysed during tracheal SMG development.

Tables

Table 1. Approximate stages of the distinct morphological events of anterior nasal gland development.

Gland Name	Approx. age of budding	Approx. age of initial lumen formation	Approx. age of onset of branching
Steno's Gland	E12.0	-	E15.5
LNG2	E13.5	E14.5-E15.0	E16.5
LNG3	E14.0-14.5	E15.0	E16.5
LNG4	E14.5	E15.5	E16.5
LNG5	E14.5	E15.5	E17.0
MNG1	E14.0	E14.5	E15.5
MNG2	E14.5	E15.5	E16.5
MNG3	E15.5	E16.5	E17.0
MNG4	E16.0	E17.5	E17.5
MSG	E14.5-E15.0	-	E15.0

Figures

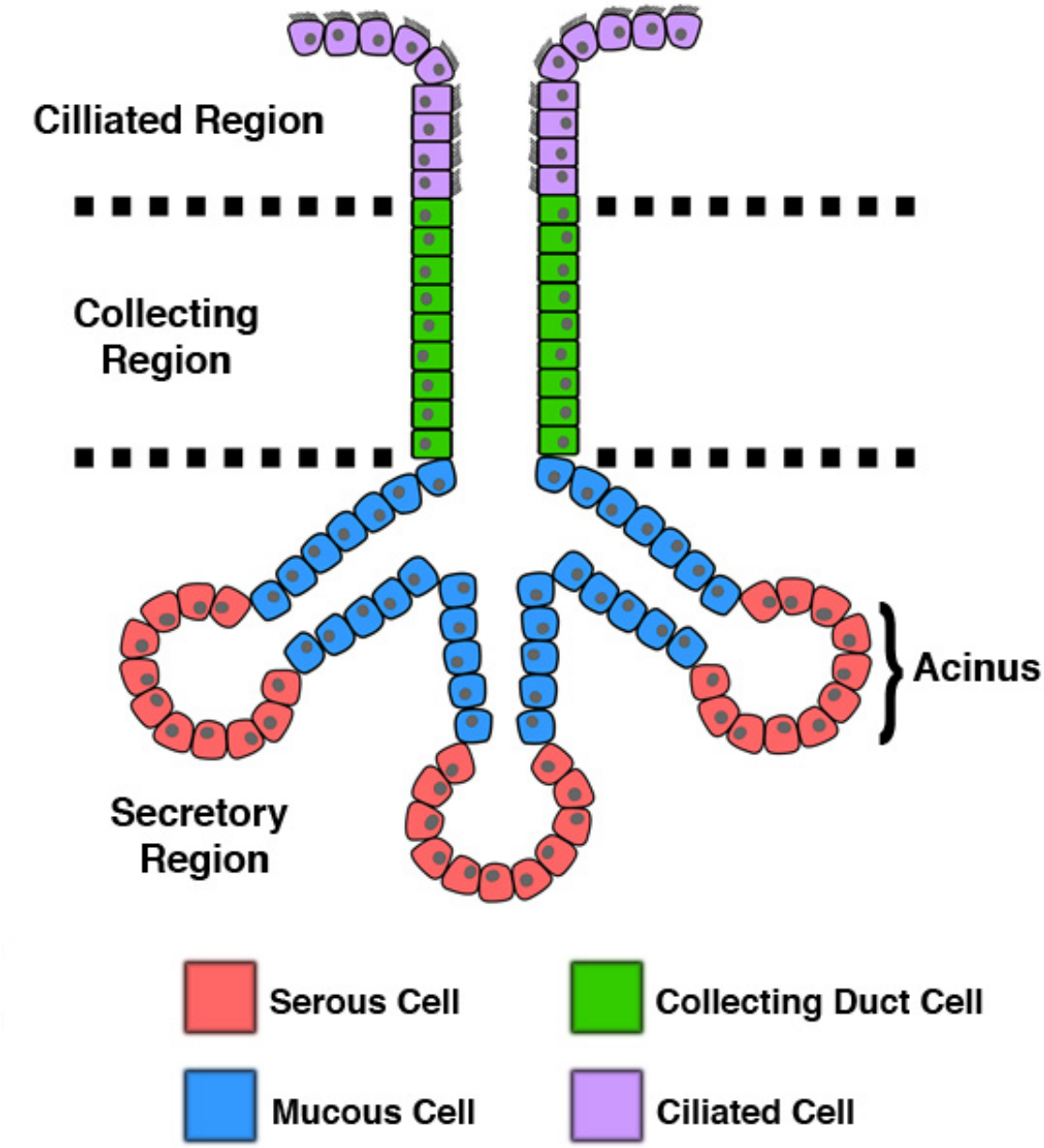

Figure 1.

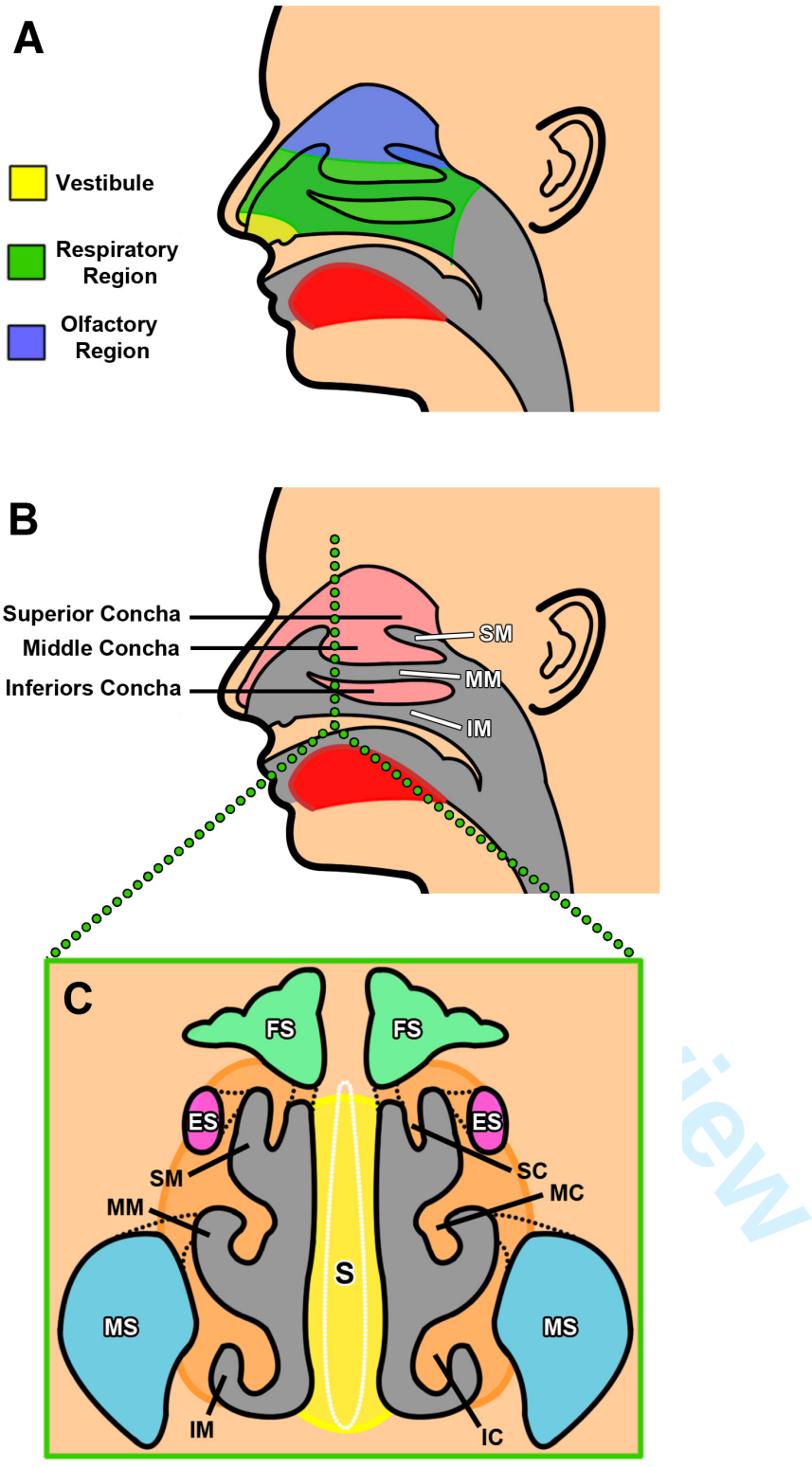
A
Vestibule
Respiratory Region
Olfactory Region
B
Superior Concha
Middle Concha
Inferiors Concha
SM
MM
IM
C
FS
FS
ES
ES
SM
SC
MM
MC
S
MS
MS
IM
IC

Figure 2.

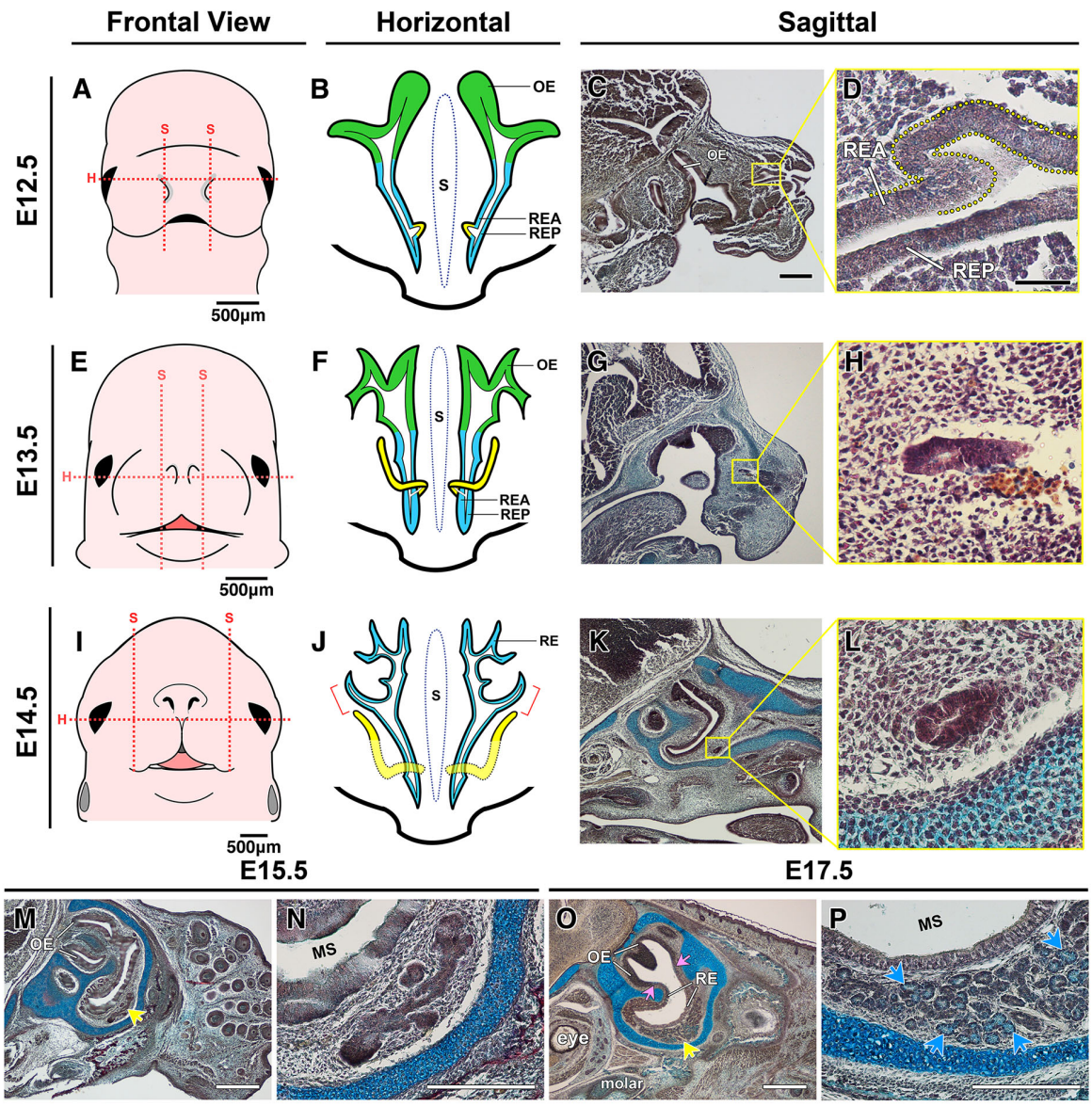
Frontal View
Horizontal
Sagittal
E12.5
E13.5
E14.5
E15.5
E17.5
A
B
C
D
E
F
G
H
I
J
K
L
M
N
O
P
S
H
OE
REA
REP
RE
MS
eye
molar
500μm

Figure 3.

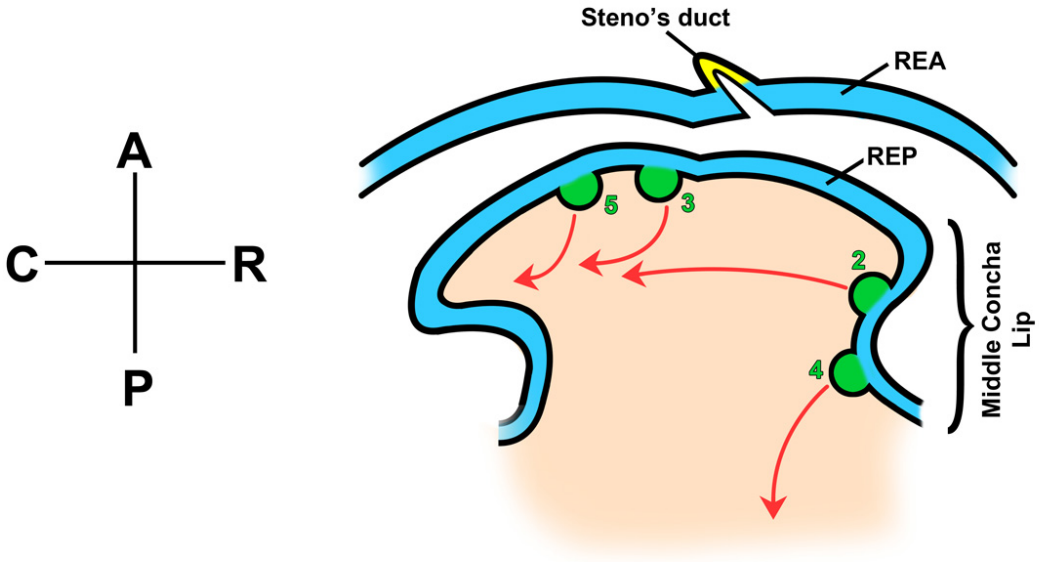

Figure 4.

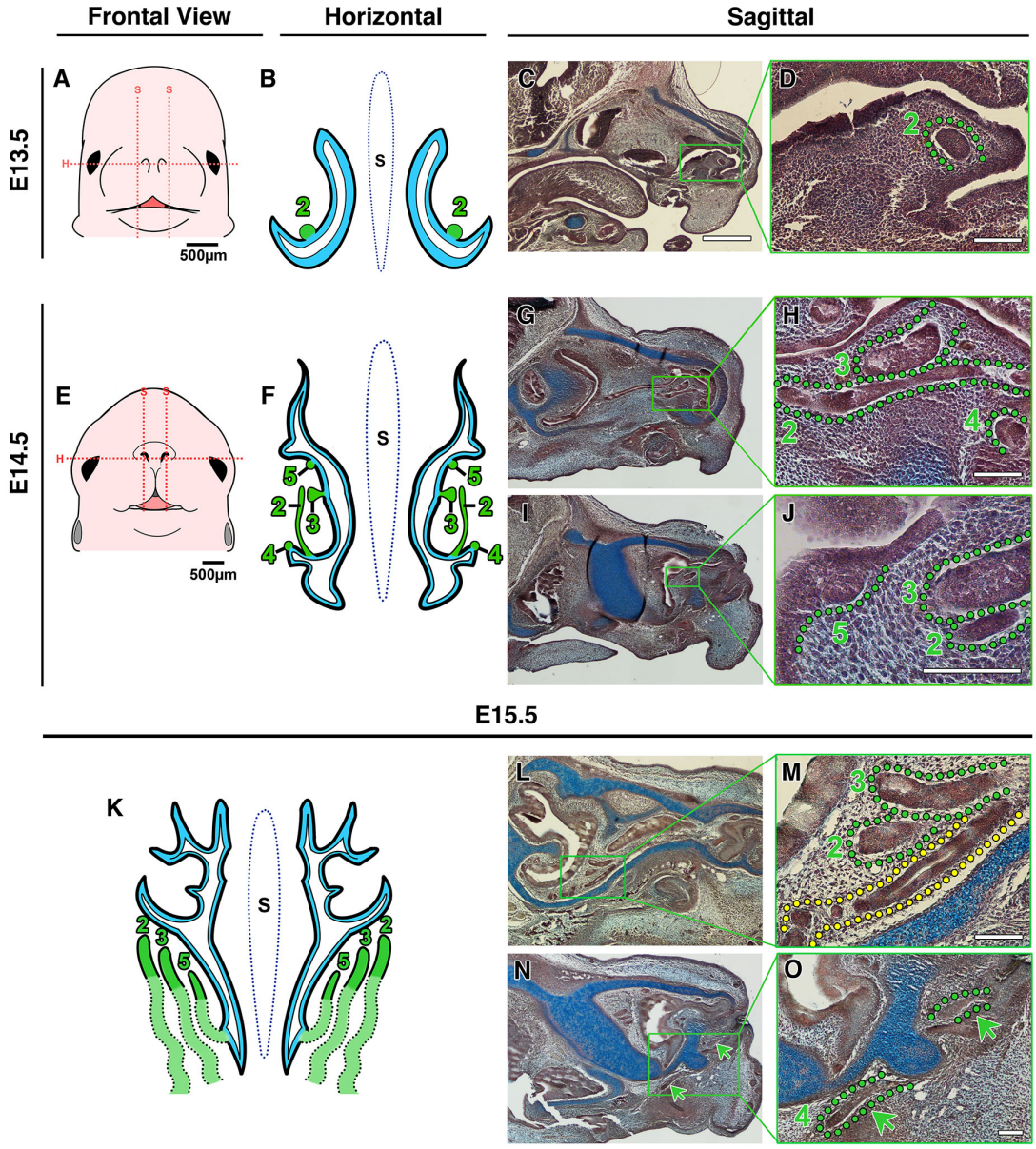
Frontal View
Horizontal
Sagittal
E13.5
E14.5
E15.5
A
B
C
D
E
F
G
H
I
J
K
L
M
N
O
S
H
500μm
2
3
4
5

Figure 5.

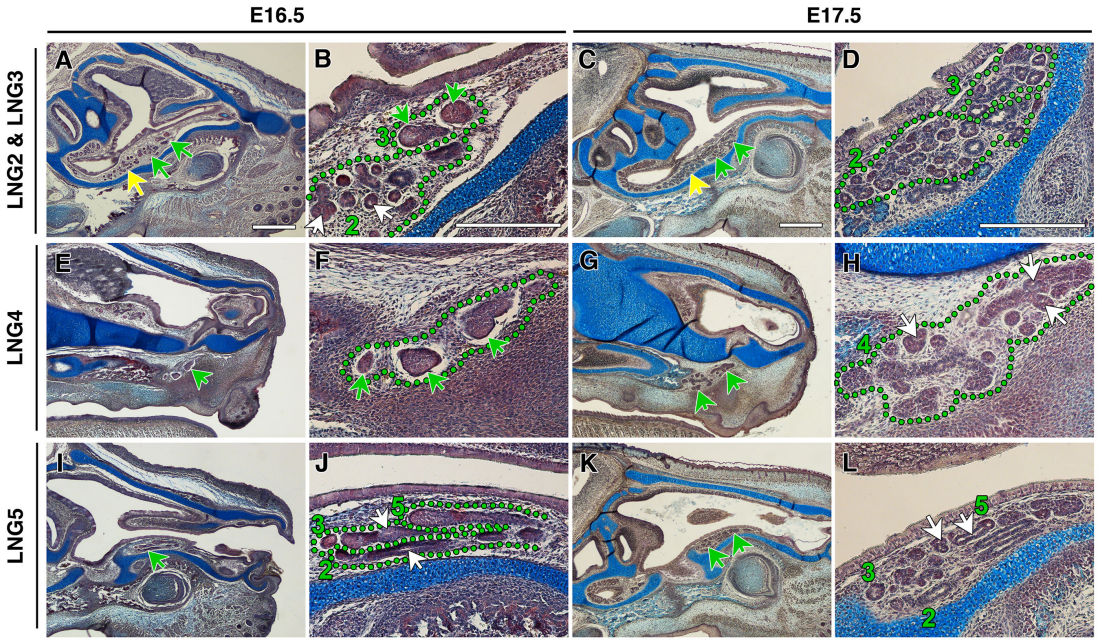

Figure 6.

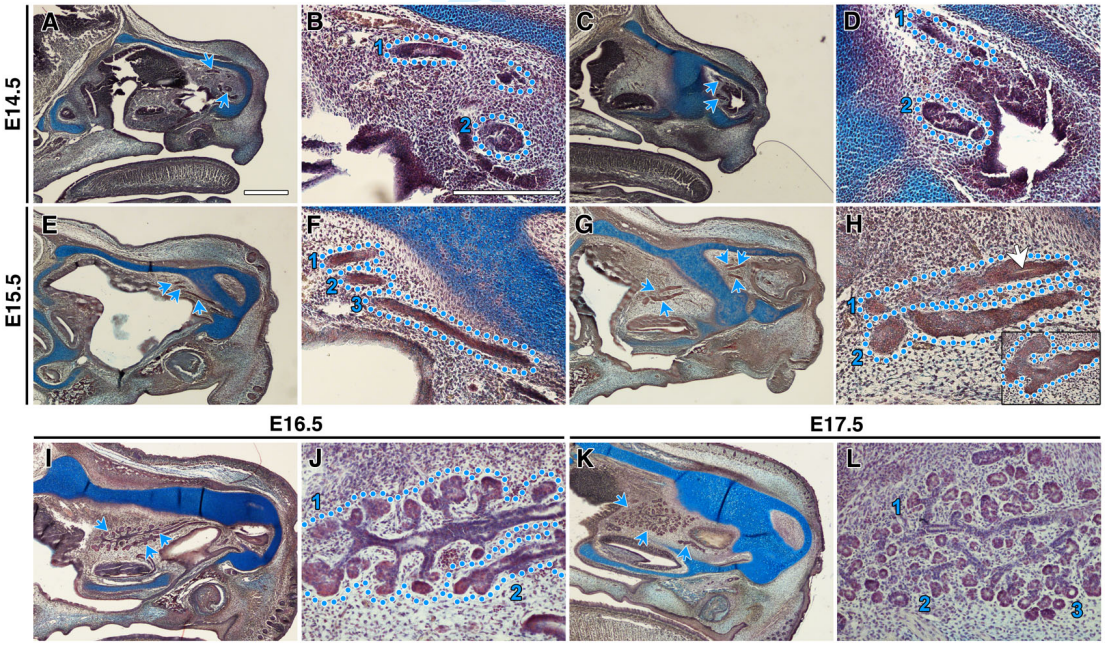

Figure 7.

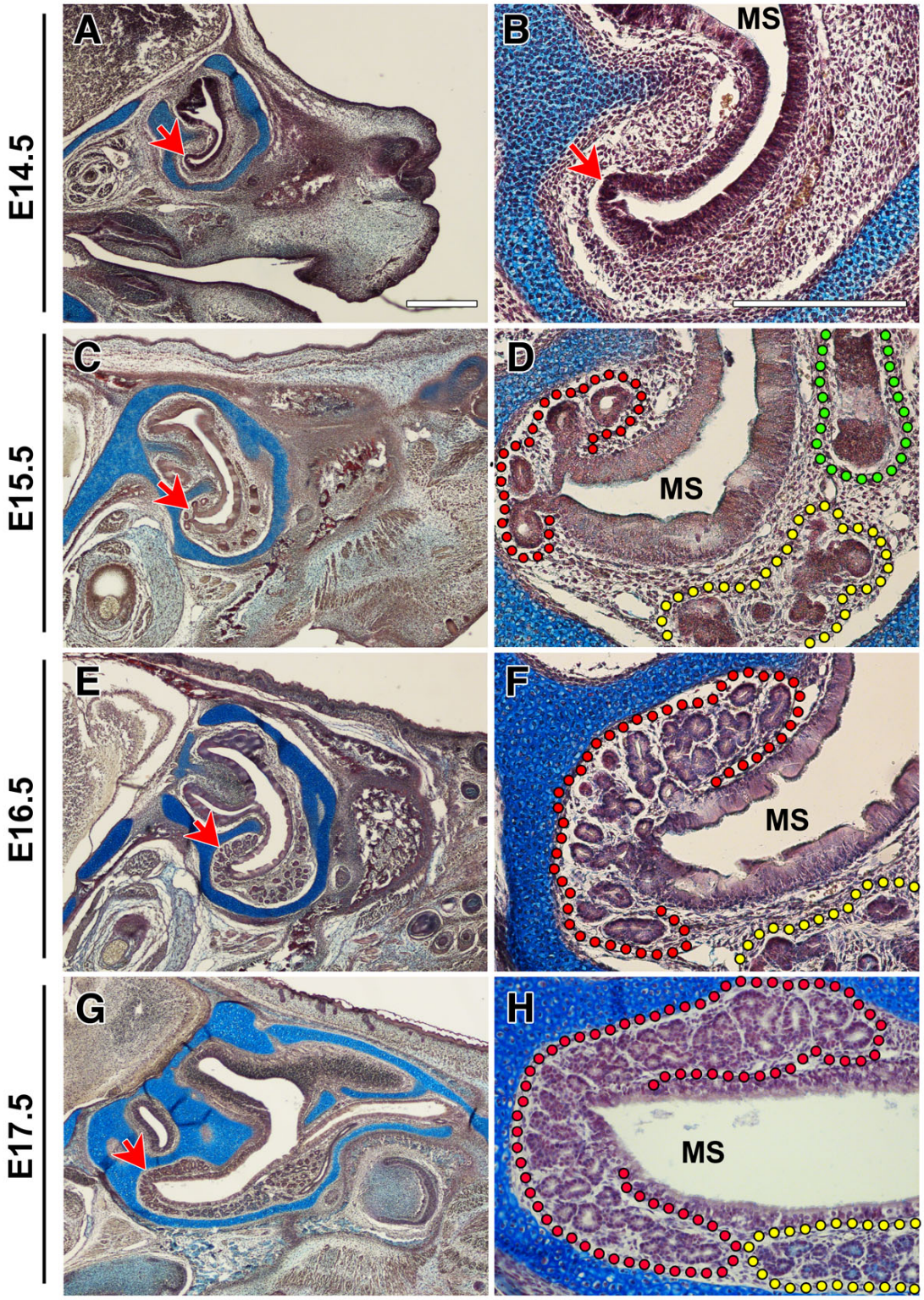

Figure 8.

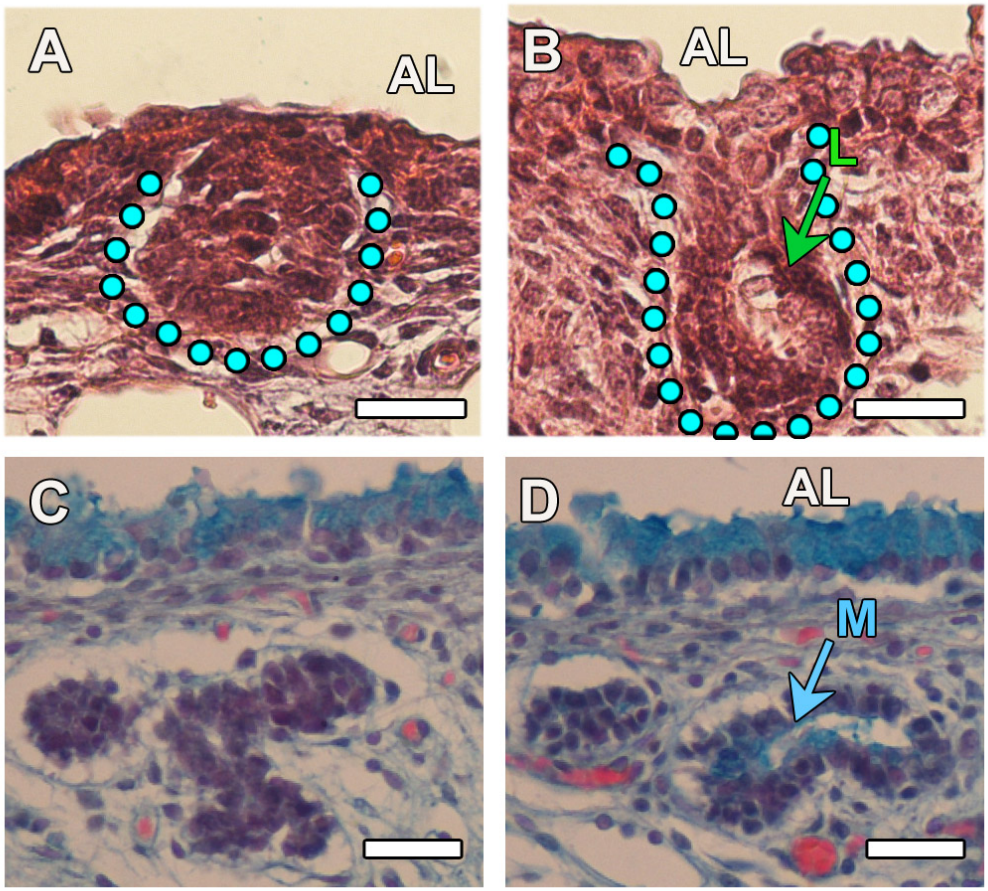

Figure 9.

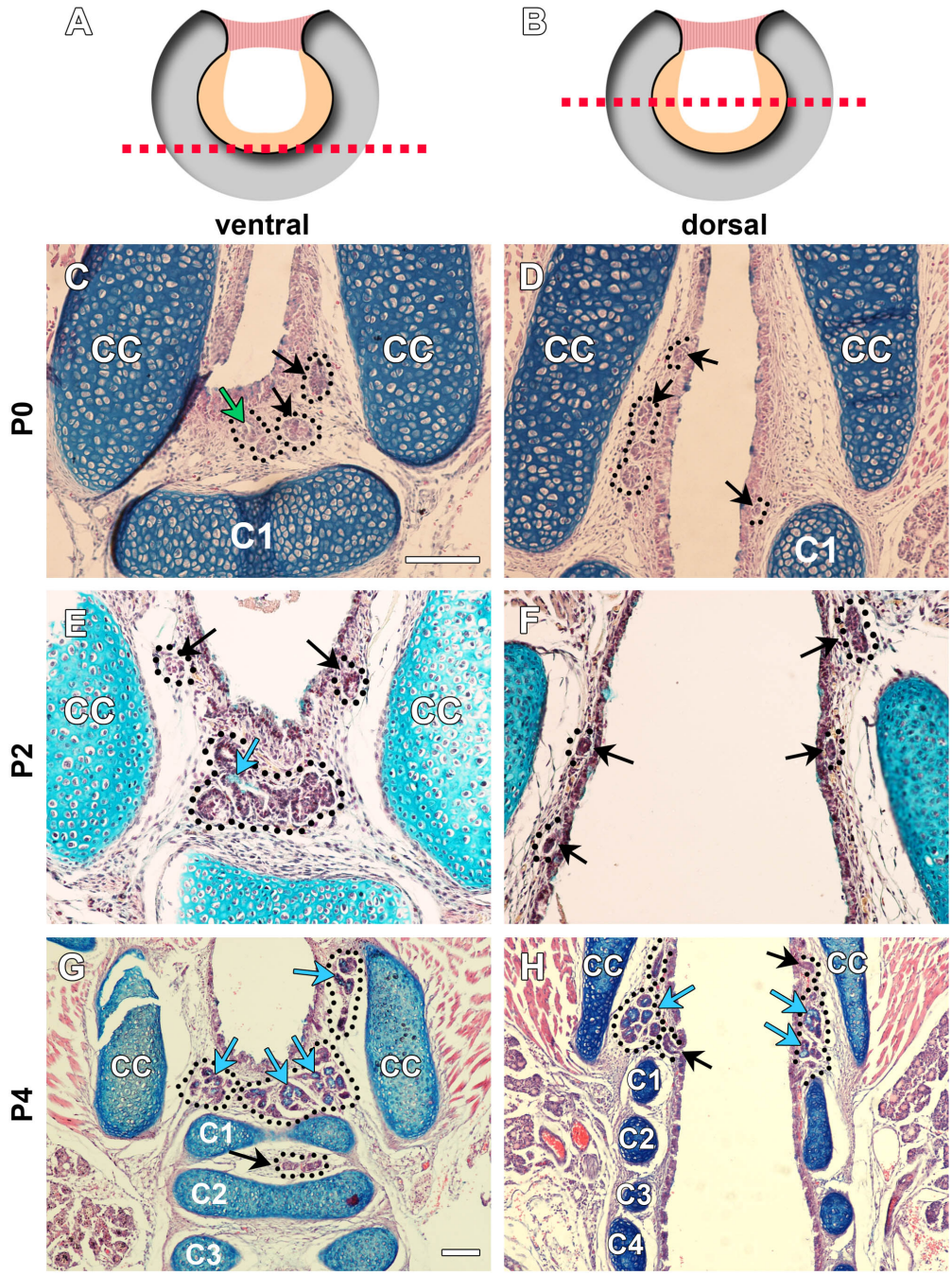

Figure 10.

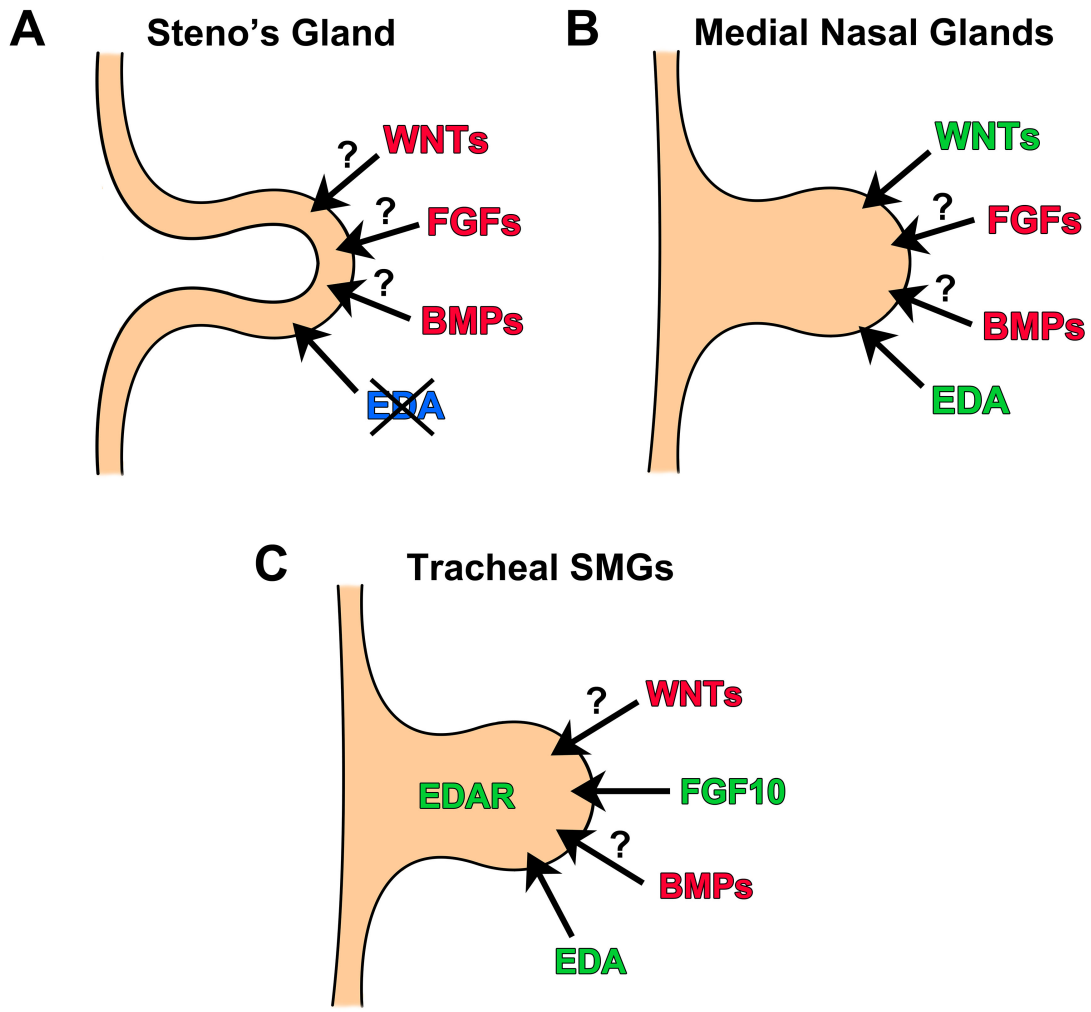

Figure 11.